Construction of Pericams

We first made a construct in which cpEYFP.1 was fused to the carboxyl terminus of M13 through a tripeptide linker SAG, and through a GTG linker to the amino terminus of a CaM mutant (Fig. 1B), in which the conserved bidentate glutamate at position 104 in the third Ca^{2+}-binding loop had been changed to glutamine (Miyawaki et al. 1997). As the amino terminus of CaM and the carboxyl terminus of M13 were rather far apart (58 Å when the complex was formed), the β-can of cpEYFP.1 might be considerably twisted. However, this radically designed chimeric protein was fluorescent and, as we had hoped, showed Ca^{2+} sensitivity. The protein, having a circularly *per*muted EYFP.1 and a *CaM*, was named "pericam." The CaM and M13 domains projecting from cpEYFP.1 reminded us of the bill of a pelican. When excited at 485 nm, Ca^{2+}-bound pericam showed an emission peak at 520 nm, which was three times more intense than that of Ca^{2+}-free pericam (data not shown).

Three types of pericams have been generated by mutating several amino acids adjacent to the chromophore (Fig. 4) (Nagai et al. 2001). Of these, "flash pericam" becomes bright in the presence of Ca^{2+}, similar to G-CaMP (Nakai et al. 2000), another cpGFP-based Ca^{2+} probe, whereas "inverse pericam" dims. A third pericam, "ratiometric pericam" has an excitation wavelength that changes in a Ca^{2+}-dependent manner, and thereby enables dual excitation ratiometric Ca^{2+} imaging. Ratiometric pericam realizes quantitative Ca^{2+} measurement by minimizing the effects of several artifacts that are unrelated to changes in free intracellular Ca^{2+} concentration ($[Ca^{2+}]_i$). This pericam has been successfully used to monitor changes in $[Ca^{2+}]_i$ in cardiomyocyte mitochondria (Robert et al. 2001). That report has demonstrated that mitochondrial $[Ca^{2+}]$ ($[Ca^{2+}]_m$) oscillates synchronously with cytosolic $[Ca^{2+}]$ during beating.

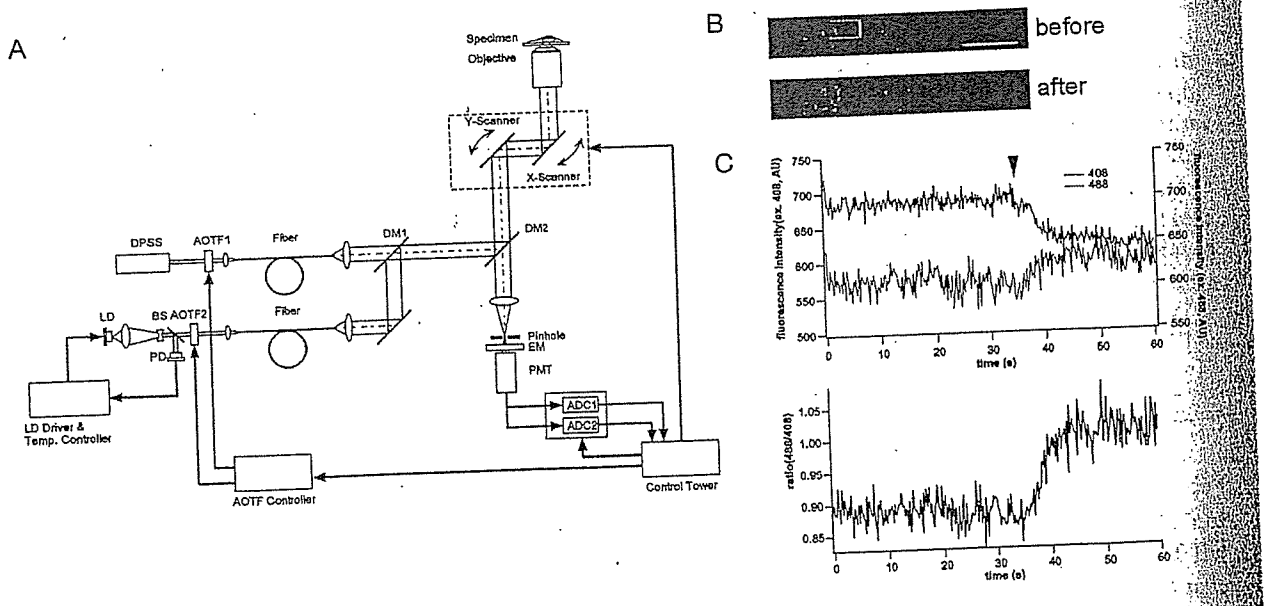

FIGURE 5. (*A*) Schematic diagram of the laser-scanning confocal microscopy system for fast dual-excitation ratiometric imaging. (DPSS) Diode-pumped solid-state laser; (LD) laser diode; (PD) photodiode; (BS) beam splitter; (DM) dichroic mirror; (EM) emission filter; (PMT) photomultiplier tube; (ADC) analog-to-digital converter. (*B*) Confocal and dual-excitation imaging of $[Ca^{2+}]_m$ using ratiometric pericam-mt. Ratio images before and after application of 1 μM histamine. Bar, 5 μm. (*C*) Time course of the averaged fluorescence signals from the white box in *B* with excitation at 488 (*green*) and 408 nm (*violet*) (*top*) and the ratio (*bottom*). The arrowhead indicates the time when histamine was applied. (Reprinted, with permission, from Shimozono et al. 2002 [©AAAS].)

Fast, Confocal Imaging of Calcium Using Ratiometric Pericam

In dual-excitation imaging, the excitation wavelength was alternated using a rotating wheel containing two band-pass filters or a high-speed grating monochromator. Use of the monochromator increased the rate at which the ratio measurement was conducted to ~10 Hz, allowing us to monitor the beat-to-beat changes in $[Ca^{2+}]_m$ of spontaneously contracting cardiac myocytes (Robert et al. 2001). These measurements were performed using conventional wide-field microscopy, which is suitable for producing the excitation peaks. However, monitoring of $[Ca^{2+}]$ change is often severely limited by the poor spatiotemporal resolution of the conventional wide-field microscopy. To obtain more reliable information on subcellular $[Ca^{2+}]$ change, it is necessary to increase the *z*-axis resolution and the rate of production and collection of the ratios of the excitation peaks. Figure 5A is a scheme for a modified laser-scanning confocal microscopy (LSCM) system for ratiometric pericam (Shimozono et al. 2002). Fast exchange between two laser beams was achieved using acousto-optic tunable filters (AOTFs). Samples were scanned on each line sequentially by a violet laser diode (408 nm) and a diode-pumped solid-state laser (488 nm). In this way, the ratios of the excitation peaks were obtained at frequencies of up to 200 Hz.

Calcium Transients in Motile Mitochondria

Although the cationic probe rhod2 has been widely used for measuring $[Ca^{2+}]_m$, the targeting specificity of this probe relies on the negative membrane potential of this organelle. On the other hand, the Ca^{2+}-sensitive photoprotein aequorin can be specifically targeted to the mitochondria and has been used for monitoring mitochondrial Ca^{2+} dynamics. However, aequorin requires the incorporation of coelenterazine, is irreversibly consumed by Ca^{2+}, and is very difficult to image because of its weak luminescence. To overcome these limitations, we have selectively targeted the ratiometric pericam to mitochondria in HeLa cells. First, changes in $[Ca^{2+}]_m$ were monitored by alternating the excitation wavelength automatically with conventional wide-field microscopy. In those studies, the excitation ratio acquisition rate was ~10 Hz, which was identical to the frame rate. Despite this high acquisition rate, the $[Ca^{2+}]_m$ measurements were often adversely affected by the rapid movement of the mitochondria, particularly at warmer temperatures. Therefore, using the modified LSCM technique, we increased the speed of excitation wavelength alteration so that it was faster than the movement of the mitochondria. With this method, the frame rate was 5 Hz and the excitation ratio-acquisition rate was 200 Hz. Although the frame rate did not allow us to fully monitor the rapid movement of the mitochondria, the high ratio-acquisition rate minimized the time lag between the two measurements used to produce each ratio signal. We believe that this $[Ca^{2+}]_m$ imaging method effectively corrects for the movement of mitochondria laterally or into and out of the optical section. After the application of histamine, spots of $[Ca^{2+}]_m$ increasing within a mitochondrion were identifiable (Fig. 5B), and the global increase in $[Ca^{2+}]_m$ was found to occur relatively slowly (Fig. 5C).

REFERENCES

Baird G.S., Zacharias D.A., and Tsien R.Y. 1999. Circular permutation and receptor insertion within green fluorescent proteins. *Proc. Natl. Acad. Sci.* **96:** 11241–11246.

Dickson R.M., Cubitt A.B., Tsien R.Y., and Moerner W.E. 1997. On/off blinking and switching behaviour of single molecules of green fluorescent protein. *Nature* **388:** 355–358.

Griesbeck O., Baird G.S., Campbell R.E., Zacharias D.A., and Tsien R.Y. 2001. Reducing the environmental sensitivity of yellow fluorescent protein. Mechanism and applications. *J. Biol. Chem.* **276:** 29188–29194.

Miyawaki A. 2003a. Fluorescence imaging of physiological activity in complex systems using GFP-based probes. *Curr. Opin. Neurobiol.* **13:** 591–596.

———. 2003b. Visualization of the spatial and temporal dynamics of intracellular signaling. *Developmental Cell* **4:** 295–305.

Miyawaki A., Griesbeck O., Heim R., and Tsien R.Y. 1999. Dynamic and quantitative Ca^{2+} measurements using improved cameleons. *Proc. Natl. Acad. Sci.* **96:** 2135–2140.

Miyawaki A., Mizuno H., Llopis J., Tsien R.Y., and Jalink K. 2000. Cameleons as cytosolic and intra-organellar calcium probes. In *Calcium Signalling: A practical approach* (ed. A.V. Tepikin), pp. 3–16. Oxford University Press, Oxford, United Kingdom.

Miyawaki A., Llopis J., Heim R., McCaffery J.M., Adams J.A., Ikura M., and Tsien R.Y. 1997. Fluorescent indicators for Ca^{2+} based on green fluorescent proteins and calmodulin. *Nature* **388:** 882–887.

Mizuno H., Sawano A., Eli P., Hama H., and Miyawaki A. 2001. Red fluorescent protein from *Discosoma* as a fusion tag and a partner for fluorescence resonance energy transfer. *Biochemistry* **40:** 2502–2510.

Nakai J., Ohkura M., and Imoto K. 2001. A high signal-to-noise Ca^{2+} probe composed of a single green fluorescent protein. *Nat. Biotechnol.* **19:** 137–141.

Nagai T., Sawano A., Park E.S., and Miyawaki A. 2001. Circularly permuted green fluorescent proteins engineered to sense Ca^{2+}. *Proc. Natl. Acad. Sci.* **98:** 3197–3202.

Nagai T., Yamada S., Tominaga T., Ichikawa M., and Miyawaki A. 2004. Expanded dynamic range of fluorescent indicators for Ca^{2+} by circularly permuted yellow fluorescent proteins. *Proc. Natl. Acad. Sci.* **101:** 10554–10559.

Nagai T., Ibata K., Park E.S., Kubota M., Mikoshiba K., and Miyawaki A. 2002. A variant of yellow fluorescent protein with fast and efficient maturation for cell-biological applications. *Nat Biotechnol.* **20:** 87–90.

Porumb T., Yau P., Harvey T.S., and Ikura M. 1994. A calmodulin-target peptide hybrid molecule with unique calcium-binding properties. *Protein Eng.* **7:** 109–115.

Robert V., Gurlini P., Tosello V., Nagai T., Miyawaki A., Di Lisa F., and Pozzan T. 2001. Beat-to-beat oscillations of mitochondrial Ca^{2+} in cardiac cells. *EMBO J.* **20:** 4998–5007.

Shimozono S., Fukano T., Nagai T., Kirino Y., Mizuno H., and Miyawaki A. 2002. Confocal imaging of subcellular Ca^{2+} concentrations using a dual-excitation ratiometric indicator based on green fluorescent protein. *Sci. STKE* **2002:** PL4. http://www.stke.org/cgi/content/full/OC_sigtrans;2002/125/pl4

Tsien R.Y. 1998. The green fluorescent protein. *Annu. Rev. Biochem.* **67:** 509–544.

———. 2000. Physiological indicators based on fluorescence resonance energy transfer. In *Imaging neurons: A laboratory manual* (ed. R. Yuste et al.), pp. 55.1–55.10. Cold Spring Harbor Laboratory Press, Cold Spring Harbor, New York.

Identification of Mitochondrial DNA Polymorphisms That Alter Mitochondrial Matrix pH and Intracellular Calcium Dynamics

An-a Kazuno[1,2☯], Kae Munakata[1☯], Takeharu Nagai[3,4¤], Satoshi Shimozono[3], Masashi Tanaka[5], Makoto Yoneda[6], Nobumasa Kato[2], Atsushi Miyawaki[3], Tadafumi Kato[1*]

1 Laboratory for Molecular Dynamics of Mental Disorders, Brain Science Institute, RIKEN, Saitama, Japan, 2 Department of Neuropsychiatry, Faculty of Medicine, University of Tokyo, Tokyo, Japan, 3 Laboratory for Cell Function and Dynamics, Brain Science Institute, RIKEN, Saitama, Japan, 4 Structure and Function of Biomolecules, Precursory Research for Embryonic Science and Technology, Japan Science and Technology Agency, Saitama, Japan, 5 Genomics for Longevity and Health, Tokyo Metropolitan Institute of Gerontology, Tokyo, Japan, 6 Second Department of Internal Medicine, University of Fukui Faculty of Medical Sciences, Fukui, Japan

Mitochondrial DNA (mtDNA) is highly polymorphic, and its variations in humans may contribute to individual differences in function as well as susceptibility to various diseases such as Parkinson disease, Alzheimer disease, bipolar disorder, and cancer. However, it is unclear whether and how mtDNA polymorphisms affect intracellular function, such as calcium signaling or pH regulation. Here we searched for mtDNA polymorphisms that have intracellular functional significance using transmitochondrial hybrid cells (cybrids) carrying ratiometric Pericam (RP), a fluorescent calcium indicator, targeted to the mitochondria and nucleus. By analyzing the entire mtDNA sequence in 35 cybrid lines, we found that two closely linked nonsynonymous polymorphisms, *8701A* and *10398A*, increased the basal fluorescence ratio of mitochondria-targeted RP. Mitochondrial matrix pH was lower in the cybrids with *8701A/10398A* than it was in those with *8701G/10398G*, suggesting that the difference observed by RP was mainly caused by alterations in mitochondrial calcium levels. Cytosolic calcium response to histamine also tended to be higher in the cybrids with *8701A/10398A*. It has previously been reported that *10398A* is associated with an increased risk of Parkinson disease, Alzheimer disease, bipolar disorder, and cancer, whereas *10398G* associates with longevity. Our findings suggest that these mtDNA polymorphisms may play a role in the pathophysiology of these complex diseases by affecting mitochondrial matrix pH and intracellular calcium dynamics.

Citation: Kazuno A, Munakata K, Nagai T, Shimozono S, Tanaka M, et al. (2006) Identification of mitochondrial DNA polymorphisms that alter mitochondrial matrix pH and intracellular calcium dynamics. PLoS Genet 2(8): e128. DOI: 10.1371/journal.pgen.0020128

Introduction

The central importance of mitochondria in ATP production is well established [1,2]. The pH gradient across the mitochondrial membrane and the inner mitochondrial membrane potential make up the electrochemical gradient, which regulates the efficiency of ATP synthesis and other mitochondrial activity. Recent studies are also focusing on the roles of mitochondria in regulation of intracellular calcium dynamics. Mitochondrial calcium uptake affects various important cellular processes such as apoptosis [3–5], exocytosis [6,7], synaptic plasticity [8], and possibly spine dynamics [9].

Mitochondria have their own DNA, mitochondrial DNA (mtDNA), which encodes the genes of 22 transfer RNAs (tRNAs), 2 ribosomal RNAs (rRNAs), and 13 subunits of enzymes related to oxidative phosphorylation [10]. Other subunits of mitochondrial proteins are encoded in the nuclear genome.

Mutations in mtDNA are known to cause various mitochondrial diseases such as mitochondrial myopathy, encephalopathy, lactic acidosis, and stroke-like episodes (MELAS), which is caused by the *3243A/G* mutation in mtDNA [11,12]. The mechanisms by which these mtDNA mutations cause functional impairment are well studied [13,14]. On the other hand, mtDNA is highly polymorphic, and certain polymorphisms are thought to be risk factors in complex diseases such as diabetes mellitus [15], Alzheimer disease [16,17], Parkinson disease [18–21], bipolar disorder [22,23], and some kinds of cancer [24,25]. It has also been reported that mtDNA polymorphisms are related to interindividual functional variability in human cognition [26], personality [27], athletic performance [28], and longevity [29]. However, these associations are solely dependent on population genetics. It is difficult to draw a definite conclusion from genetic association analyses alone because the high variability of mtDNA

Editor: Harry Orr, University of Minnesota, United States of America

Received June 17, 2005; **Accepted** June 28, 2006; **Published** August 11, 2006

DOI: 10.1371/journal.pgen.0020128

Abbreviations: cybrid, transmitochondrial hybrid cell; mt DsRed, mitochondria-targeted red fluorescent protein from *Discosoma*; mt pH-GFP, mitochondria-targeted pH-sensitive green fluorescent protein; mtDNA, mitochondrial DNA; mtRP, ratiometric Pericam targeted to mitochondria; mtSNPs, mitochondrial DNA single nucleotide polymorphisms; nucRP, ratiometric Pericam targeted to nucleus; RP, ratiometric Pericam; rRNA, ribosomal RNA; tRNA, transfer RNA

* To whom correspondence should be addressed. E-mail: kato@brain.riken.jp

☯ These authors contributed equally to this work.

¤ Current address: Laboratory of Nanosystems Physiology, Research Institute for Electronic Science, Hokkaido University, Hokkaido, Japan

Synopsis

Mitochondria play important roles in energy production and regulation of intracellular calcium levels. Mitochondria have their own genetic material, mitochondrial DNA (mtDNA). In spite of its short length (16 kbp), mtDNA is highly variable among individuals and is thought to contribute to interindividual functional variability in energy-requiring activities such as intelligence and athletic performance. However, it is unclear whether mtDNA polymorphisms affect intracellular function and condition. Using transmitochondrial hybrid cells, the authors found two closely linked mtDNA polymorphisms, *10398A/G* and *8701A/G*, which cause alterations in mitochondrial pH and calcium concentration. Cytosolic calcium response to histamine tended to be different between transmitochondrial hybrid cells carrying these two mtDNA polymorphisms. It has been reported that the *10398A* mtDNA polymorphism is a risk factor for Parkinson disease, Alzheimer disease, cancer, and bipolar disorder, whereas *10398G* is associated with longevity. The present findings suggest that these mtDNA polymorphisms may play a role in the pathophysiology of these complex diseases by affecting mitochondrial matrix pH and intracellular calcium dynamics.

among individuals makes such analysis susceptible to confounding effects of population stratification; in addition, the effects of other polymorphisms in mitochondrial or nuclear genes are difficult to control. Although functional analyses of these polymorphisms are needed, to date there are few reports that identify functional effects of mtDNA polymorphisms. This is mainly due to methodological difficulties, as conventional molecular biological techniques are not readily applicable to mtDNA.

We examined the phenotypic effect of mitochondrial DNA without interference from nuclear genes by analysing transmitochondrial hybrid cells (cybrids), which were made by fusing a cell line lacking mtDNA, called ρ^0 (rho zero) cells [30], with platelets from humans. Although the consequences of pathogenic mtDNA mutations have been examined using this technique, the functional significance of mtDNA polymorphisms has not been well investigated yet.

In this study, we searched for functional mtDNA polymorphisms using the following strategies: (1) by targeting a calcium indicator, ratiometric Pericam (RP) [31], to mitochondria and the nucleus in the same cell, mitochondrial and cytosolic calcium levels were monitored simultaneously; (2) to reduce cellular variability, a ρ^0 cell line was subcloned before generation of cybrids; (3) by sequencing the whole mtDNA genome in 35 cybrids, functional mtDNA polymorphisms were comprehensively analyzed, and two nonsynonymous mtDNA polymorphisms, *10398A/G* and *8701A/G*, were identified; and (4) using a pH indicator, we confirmed that these mtDNA polymorphisms altered both mitochondrial matrix pH and intracellular calcium levels.

Results

Generation and Confirmation of Cybrid Cell Lines

First, we established a 143B.TK$^-$ $\rho^0$206 cell line that stably expresses two RPs. RP is a ratiometric fluorescent protein developed as a calcium indicator [31]. The fluorescence ratio of 510 nm emission at 480 nm excitation to that at 410 nm excitation is reported to reflect calcium concentration at a constant pH. Mitochondria-targeted RP is also sensitive to pH because there is a higher pH [32,33] in the mitochondrial matrix (approximately 7.7–8.0) [34,35] than in the cytosol. In this study, two RPs, one targeted to mitochondria (mtRP) and the other to the nucleus (nucRP), were expressed in the same living cell. Thus, we were able to simultaneously monitor mitochondrial and cytosolic calcium concentrations [31]. Because calcium levels in the nucleus were reported to be similar to those in cytosol, nuclear calcium levels were used to indicate cytosolic calcium level.

We subcloned several ρ^0 cell lines carrying RPs and selected one that showed a reproducible calcium response. We confirmed by mtDNA-specific PCR and Southern blot analysis that this cell line lacked mtDNA. We fused this cell line with platelets taken from 35 human volunteers and confirmed the integration of mtDNA from the volunteers by Southern blot analysis.

Measurements of Fluorescence Ratio of mtRP in all Cybrid Cell Lines

Using these cybrids, we measured fluorescence ratios of mtRP and nucRP. In fluorescent images of cybrids, mitochondria had a higher 480 nm/410 nm ratio than the nucleus (Figure 1A), possibly reflecting higher calcium levels and pH in mitochondrial matrix than in cytosol. This result is consistent with previous observations in HeLa cells [32]. At first, baseline fluorescence ratios were recorded for 2 minutes. Subsequently, cells were stimulated by 10 μM histamine, which elicits inositol trisphosphate–mediated calcium release from the endoplasmic reticulum [36]. In the first 60 s following stimulation, the fluorescence ratio of mtRP and nucRP initially increased and then returned to basal levels (Figure 1B). The mtRP fluorescence ratio was measured in 11–42 cells for each of the 35 cell lines by fluorescent microscopy.

Using a one-way analysis of variance, we tested whether or not interindividual variation of mtDNA causes differences in basal mtRP fluorescence ratios. A statistically significant variation of basal mtRP fluorescence ratios was found among these cybrid lines ($p < 0.001$, $F = 6.328$).

Entire Sequences of mtDNA in All Cybrid Cell Lines

To identify the mtDNA polymorphisms that cause heterogeneity among cybrids, we determined the entire 16.5-kbp sequence of mtDNA in each of the 35 cybrids. mtDNA polymorphisms were selected in comparison with the revised Cambridge Reference Sequence [10,37]. A total of 216 polymorphic sites, including 13 novel polymorphisms, were identified. All cybrids had different sequences.

Identification of mtDNA Polymorphisms Altering the Fluorescence Ratio of mtRP

To identify the polymorphisms with functional significance, all nonsynonymous polymorphisms or polymorphisms in tRNA or rRNA found in more than three cybrids ($n = 16$) were selected (Table 1). For each polymorphism, the average mtRP fluorescence ratios for two genotypes at the particular polymorphic site were compared (Table 1). The polymorphisms at only two positions, 8701 and 10398, showed nominally significant differences of basal mtRP fluorescence ratios. Basal mtRP fluorescence ratios in cybrids with mtDNA *10398A* were significantly higher than those with *10398G*

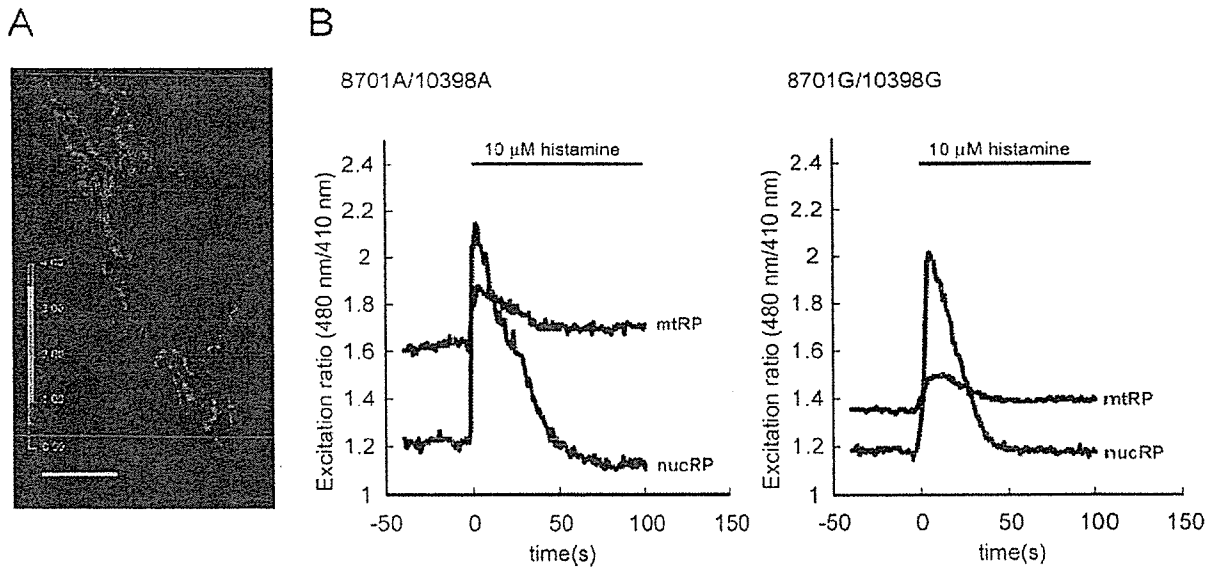

Figure 1. Typical Excitation Ratio Image of a Cybrid and Histograms Showing Responses to Histamine

(A) Image of a typical cybrid showing fluorescence ratios of excitation at 480 nm to 410 nm in pseudocolors. Mitochondria had a higher 480 nm/410 nm ratio than the nucleus, possibly reflecting higher calcium levels and pH in mitochondrial matrix than in cytosol. Scale bar, 10 μm.

(B) Representative fluorescence ratio responses of *8701A/10398A* cybrids (left) and *8701G/10398G* cybrids (right) evoked by 10 μM histamine. The *y* axis shows the ratio of the 525 nm fluorescence at 480 nm to that at 410 nm. Blue traces show the ratio in the nucleus and red traces show the ratio in mitochondria. Histamine (10 μM) was added at time 0 s and was not washed out during the experiment.

DOI: 10.1371/journal.pgen.0020128.g001

(*10398A*, 1.67 ± 0.09 [mean ± SD], $n = 11$; *10398G*, 1.59 ± 0.12 [mean ± SD], $n = 24$; $p < 0.05$, Mann-Whitney *U* test). Basal mtRP fluorescence ratios in the cybrids with *8701A* were also significantly higher than those with *8701G* (*8701A*, 1.67 ± 0.1 [mean ± SD], $n = 13$; *8701G*, 1.59 ± 0.11 [mean ± SD], $n = 22$; $p < 0.05$). Because *8701A* was linked to *10398A* in all but two cybrids, it was difficult to assess the independent effects of these polymorphisms. Since these two cybrids showed intermediate values (average fluorescence ratio, 1.64), it suggests that both of these polymorphisms may contribute to the observed difference. Because there were only two subjects with *8701G/10398A*, further analyses were performed using only *8701A/10398A* and *8701G/10398G* cybrids.

Basal mtRP fluorescence ratios in cybrids with *8701A/10398A* mtDNA were significantly higher than those with *8701G/10398G* mtDNA (*8701A/10398A*, 1.67 ± 0.09 [mean ± SD], $n = 11$; *8701G/10398G*, 1.59 ± 0.11 [mean ± SD], $n = 22$; $p < 0.05$, Mann-Whitney *U* test; Figures 1 and 2). Peak mtRP fluorescence ratios after the histamine stimulation also showed a similar but nonsignificant trend (*8701A/10398A*, 1.86 ± 0.11 [mean ± SD]; *8701G/10398G*, 1.78 ± 0.14 [mean ± SD]; $p = 0.05$).

Replication Study Using Cybrid Cell Lines Stably Expressing RP

Because the nominally significant effects of polymorphisms at positions 10398 and 8701 on basal mtRP fluorescence ratio were found after multiple statistical analyses, we performed a second study to ensure it was not a false-positive finding. Three cybrid lines with *8701A/10398A* mtDNA and three with *8701G/10398G* mtDNA were chosen from among the 35 cybrids for the replication study (Table S1). The results confirmed our initial observation of a higher basal mtRP fluorescence ratio in cybrids with mtDNA *8701A/10398A* (*8701A/10398A*, 1.78 ± 0.04 [mean ± SD], three cell lines; *8701G/10398G*, 1.67 ± 0.01 [mean ± SD], three cell lines). Peak mtRP fluorescence ratios after the histamine stimulation also showed a similar trend (*8701A/10398A*, 1.99 ± 0.04 [mean ± SD], three cell lines; *8701G/10398G*, 1.88 ± 0.02 [mean ± SD], three cell lines).

Replication Study Using Independently Established Cybrid Cell Lines

To further confirm that the observed difference is caused by the difference of mtDNA sequence, we performed another replication study using independently established cybrid cell lines. In this experiment, the native 143B.TK$^-$ $\rho^0$206 cell line was used without any further subcloning. We established independent cybrid cell lines by using platelets derived from a subgroup of the original 35 donors (Table S1). By transiently transfecting the cybrids with *ratiometric coxIV-Pericam* cDNA, fluorescence imaging was performed. Moreover, cells were stimulated by 10 μM histamine, and in vivo calibration was performed using calibration buffers with ionomycin, which equilibrate intramitochondrial and extracellular calcium. To minimize the cell-to-cell variability, an index for calcium level, $(R - R_{min}) / (R_{max} - R)$ (see Materials and Methods), was analyzed in cells responded to histamine. As a result, our initial observation in cybrids with mtDNA *8701A/10398A* was confirmed (*8701A/10398A*, 1.07 ± 0.40 [mean ± SD], three cell lines; *8701G/10398G*, 0.51 ± 0.09 [mean ± SD], three cell lines; Figure S1).

Generation of pH Indicator for Measurements of Mitochondrial Matrix pH

It has been reported that the fluorescence ratio of RP is dependent not only on calcium levels but also on pH [32,33],

Table 1. The mtDNA Polymorphisms in 35 Cybrids

Nucleotide Change	Gene[a]	Amino Acid Change[b]	Number of Subjects[c]		Basal Fluorescence Ratio of Mitochondria-Targeted RP[f]		Statistical Analysis[g]	Disease Related[h]
			Anderson Sequence[d]	Non-Anderson Sequence[e]	Anderson Sequence	Non-Anderson Sequence	*p*	
A633T	tRNA Pro		34	1	—	—	—	
A663G	12S rRNA		31	4	1.61	1.70	0.213	
G709A	12S rRNA		30	5	1.63	1.58	0.962	
A750G	12S rRNA		0	35	—	—	—	
C752T	12S rRNA		34	1	—	—	—	
A827G	12S rRNA		32	3	1.62	1.65	—	
C922T[i]	12S rRNA		34	1	—	—	—	
T1107C	12S rRNA		34	1	—	—	—	
C1310T	12S rRNA		33	2	—	—	—	DM
A1382C	12S rRNA		34	1	—	—	—	
T1413C	12S rRNA		34	1	—	—	—	
A1438G	12S rRNA		1	34	—	—	—	DM
G1442A	12S rRNA		34	1	—	—	—	
T1452C	12S rRNA		34	1	—	—	—	
G1598A	12S rRNA		34	1	—	—	—	
A1736G	16S rRNA		31	4	1.61	1.70	0.213	
A2109T[i]	16S rRNA		34	1	—	—	—	
T2150-51TA[j]	16S rRNA		31	4	1.61	1.70	0.213	
T2404C	16S rRNA		34	1	—	—	—	
T2626C	16S rRNA		30	5	1.62	1.59	0.480	
A2706G	16S rRNA		1	34	—	—	—	
C2766T	16S rRNA		34	1	—	—	—	
C2772T	16S rRNA		30	5	1.62	1.59	0.480	
G2831A	16S rRNA		34	1	—	—	—	
G3010A	16S rRNA		24	11	1.62	1.62	0.749	
C3204T	16S rRNA		34	1	—	—	—	
C3206T	16S rRNA		32	3	1.62	1.65	—	
G3391A	ND1	G29S	34	1	—	—	—	
A3434G	ND1	Y43C	34	1	—	—	—	
T3644C	ND1	V113A	34	1	—	—	—	
G4048A	ND1	D248N	33	2	—	—	—	
T4386C	tRNA Gln		30	5	1.62	1.59	0.480	
A4824G	ND2	T119A	31	4	1.61	1.70	0.213	
A4833G	ND2	T122A	32	3	1.63	1.46	—	
C5178A	ND2	L237M	23	12	1.62	1.62	0.677	
C5263T	ND2	A265V	34	1	—	—	—	
A5301G	ND2	I278V	34	1	—	—	—	
T5418C	ND2	F317L	33	2	—	—	—	
G5460A	ND2	A331T	32	3	1.63	1.48	—	AD, PD
G5773A	tRNA Cys		33	2	—	—	—	
A6040G	COI	N46S	34	1	—	—	—	
C6318T[i]	COI	P139S	34	1	—	—	—	
G7269A[i]	COI	V456M	34	1	—	—	—	
T7270C	COI	V456A	34	1	—	—	—	
T7297C[i]	COI	V465A	34	1	—	—	—	
G7444A	COI	Ter514K	34	1	—	—	—	LHON, SNHL
G7521A	tRNA Asp		34	1	—	—	—	
G7664A	COII	A27T	34	1	—	—	—	
A7673G	COII	T30V	34	1	—	—	—	
G7853A	COII	V90I	33	2	—	—	—	
G7859A	COII	D92N	34	1	—	—	—	
C8414T	ATP8	L17F	24	11	1.62	1.62	0.749	
A8563G	ATP6	T13A	31	4	1.61	1.70	0.213	
G8584A	ATP6	A20T	34	1	—	—	—	
A8701G	ATP6	T59A	13	22	1.67	1.59	**0.037**	
G8764A	ATP6	A80T	34	1	—	—	—	
C8794T	ATP6	H90Y	31	4	1.61	1.70	0.213	
A8860G	ATP6	T112A	0	35	—	—	—	
C9011T[i]	ATP6	A162V	34	1	—	—	—	
A9355G	COIII	N50S	34	1	—	—	—	
G9477A	COIII	V91I	34	1	—	—	—	
A9670G	COIII	N155S	34	1	—	—	—	
T10345C	ND3	I96T	33	2	—	—	—	
A10398G	ND3	T114A	11	24	1.67	1.59	**0.036**	
T10410C	tRNA Arg		32	3	1.62	1.65	—	

Table 1. Continued

Nucleotide Change	Gene[a]	Amino Acid Change[b]	Number of Subjects[c]		Basal Fluorescence Ratio of Mitochondria-Targeted RP[f]		Statistical Analysis[g]	Disease Related[h]
			Anderson Sequence[d]	Non-Anderson Sequence[e]	Anderson Sequence	Non-Anderson Sequence	*p*	
G10427A	tRNA Arg		34	1	—	—	—	
G11016A	ND4	S86N	34	1	—	—	—	
A11084G	ND4	T109A	30	5	1.62	1.59	0.480	MELAS
T11255C	ND4	Y166H	34	1	—	—	—	
A12026G	ND4	I423V	34	1	—	—	—	DM
C12135T	ND4	S459F	33	2	—	—	—	
G12236A	tRNA Ser		34	1	—	—	—	
A12358G	ND5	T8A	32	3	1.62	1.65	—	
A12361G	ND5	T9A	34	1	—	—	—	
T12811C	ND5	Y159H	33	2	—	—	—	
T12880C	ND5	F182L	33	2	—	—	—	
A13651G	ND5	T439A	34	1	—	—	—	
G13928A	ND5	S531N	34	1	—	—	—	
A13942G	ND5	T536A	33	2	—	—	—	
A14053G	ND5	T573A	34	1	—	—	—	
T14178C	ND6	I166V	34	1	—	—	—	
A14693G	tRNA Glu		34	1	—	—	—	
A14696G	tRNA Glu		34	1	—	—	—	
C14766T	Cytb	T7I	0	35	—	—	—	
G14858A	Cytb	G38S	34	1	—	—	—	
T14979C	Cytb	I78T	32	3	1.62	1.65	—	
A15218G	Cytb	T158A	34	1	—	—	—	
A15236G	Cytb	I164V	34	1	—	—	—	
G15314A	Cytb	A190T	34	1	—	—	—	
G15323A	Cytb	A193T	33	2	—	—	—	
A15326G	Cytb	T194A	0	35	—	—	—	
C15468T[i]	Cytb	T241M	34	1	—	—	—	
T15479C	Cytb	F245L	34	1	—	—	—	
G15497A	Cytb	G251S	33	2	—	—	—	PIEI
A15662G	Cytb	I306V	34	1	—	—	—	
A15758G	Cytb	T338V	34	1	—	—	—	
A15851G	Cytb	I369V	34	1	—	—	—	
A15860G	Cytb	I372V	33	2	—	—	—	
A15901G[i]	tRNA Thr		34	1	—	—	—	
G15927A	tRNA Thr		34	1	—	—	—	
G15930A	tRNA Thr		33	2	—	—	—	
T15940C	tRNA Thr		34	1	—	—	—	
G16000A	tRNA Pro		34	1	—	—	—	

Boldface entries, $p < 0.05$.

[a]ND1, ND2, ND3, ND4, ND5, ND6, genes encoding subunits of complex I (NADH dehydrogenase); COI, COII, COIII, subunits of complex IV (cytochrome *c* oxidase); ATP8, ATP6, subunits of complex V (ATP synthase); and Cytb, a subunit of complex III (ubiquinol: cytochrome *c* oxidoreductase).

[b]For example, G29S means that the G3391A causes substitution from glycine (G) to serine (S) at the 29th amino acid of the ND1 gene.

[c]The number of subjects among 35 cybrids.

[d]The revised Cambridge Reference Sequence.

[e]Only the bases that differed from Anderson sequence are shown.

[f]Each value indicates the excitation ratio (480 nm/410 nm).

[g]Mann-Whitney *U* test was applied only when the number of subjects in both groups were larger than three.

[h]The polymorphisms denoted as "disease related" in the MITOMAP database, a human mitochondrial genome database (http://www.mitomap.org).

[i]Polymorphisms newly identified in this study.

[j]Insertion.

AD, Alzheimer disease; DM, diabetes mellitus; LHON, Leber hereditary optic neuropathy; MELAS, mitochondrial encephalomyopathy, lactic acidosis, and stroke-like episodes; SNHL, sensorineuronal hearing loss; PIEI, paracrystalline inclusions with exercise intolerance.

DOI: 10.1371/journal.pgen.0020128.t001

especially at the higher pH range found in the mitochondrial matrix. To test the relative contributions of these factors to the observed finding, we attempted to measure mitochondrial pH using mitochondria-targeted, pH-sensitive green fluorescent protein (mt pH-GFP) [38,39] and mitochondria-targeted red fluorescent protein from *Discosoma* (mt DsRed) expressed under the control of a bidirectional promoter [40–42]. Because the pKa of pH-GFP is approximately 8.0, it is useful for measuring mitochondrial matrix pH. Since DsRed is a pH-insensitive protein, it can be used as a reference [43].

We confirmed that this pH indicator, mt pH-GFP/DsRed, could be successfully used to measure mitochondrial pH.

Measurements of Mitochondrial Matrix pH in Cybrids with mtDNA *8701A/10398A* and *8701G/10398G*

For the measurements of mitochondrial matrix pH, we used the above-mentioned independently established lines of

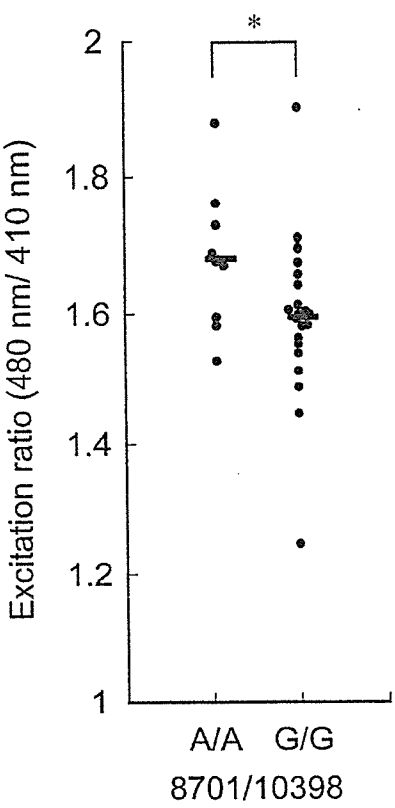

Figure 2. Effects of *10398A/G* on Basal Fluorescence Ratios of Mitochondria-Targeted RP

Differences between the basal fluorescence ratios in *10398A* and *10398G* cybrids are shown. All cybrids with *8701A* have *10398A* (left). While most cybrids with *8701G* had *10398G* (right), two cybrids had *8701A* and *10398G* (the data of these two cybrids were 1.52 and 1.77). For each cybrid, data taken from 11–42 cells (average, 26 cells) were averaged. The *y* axis shows the ratio of the 525 nm fluorescence at 480 nm to that at 410 nm. Horizontal bars indicate the mean values for each type of cybrid. $^*p < 0.05$ (Mann-Whitney *U* test).

DOI: 10.1371/journal.pgen.0020128.g002

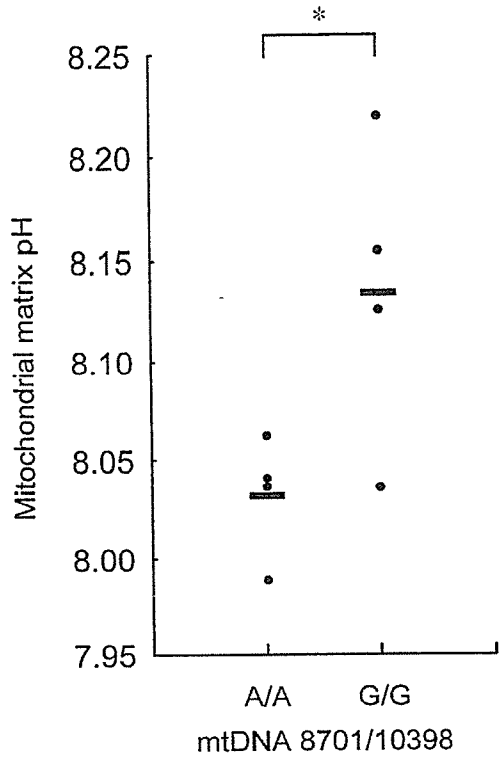

Figure 3. Basal Mitochondrial Matrix pH in the Cybrids with *8701A/10398A* or *8701G/10398G*

Data from 11–18 cells in a triplicate experiment were averaged for each of four cell lines in each group. The *y* axis shows mitochondrial matrix pH calculated by calibration in vivo. Horizontal bars indicate the mean values for each type of cybrid. $^*p < 0.05$ (*t* test).

DOI: 10.1371/journal.pgen.0020128.g003

cybrids generated from the native 143B.TK$^-$ ρ^0 206 cell line that does not carry RPs (four with *8701A/10398A* and four with *8701G/10398G*). By transiently cotransfecting the mt pH-GFP/DsRed and Tet-Off vectors, basal mitochondrial matrix pH was recorded for several minutes in each cybrid cell line. We performed in vivo calibration of mitochondrial basal matrix pH in each cell by using four calibration buffers (pH 7.0, 7.5, 8.0, and 8.5) with the ionophores nigericin and monensin, which equilibrate intramitochondrial and extracellular pH. The calculated basal mitochondrial matrix pH was about 8.0, which is consistent with previous reports using HeLa cells and ECV304 cells [34,35]. Compared with the *8701G/10398G* cybrids, the basal mitochondrial matrix pH was significantly lower in the *8701A/10398A* cybrids (*8701A/10398A*, 8.03 ± 0.03 [mean ± SD], four cell lines; *8701G/10398G*, 8.13 ± 0.07 [mean ± SD], four cell lines; $p < 0.05$, *t* test; Figure 3).

Cytosolic Calcium Dynamics

To test whether or not these mtDNA polymorphisms affect cytosolic calcium dynamics, we examined the effects of *8701A/10398A* and *8701G/10398G* genotypes on the cytosolic calcium levels.

The nucRP data from the first experiments indicated that the *8701A/10398A* cybrids tended to have higher peak cytosolic calcium levels after the histamine stimulation compared with the *8701G/10398G* cybrids (*8701A/10398A*, 2.10 ± 0.14 [mean ± SD], 11 cell lines; *8701G/10398G*, 2.02 ± 0.15, 22 cell lines, [mean ± SD]; $p = 0.08$, Mann-Whitney *U* test; Figure 4). There was no significant difference of basal cytosolic calcium level (*8701A/10398A*, 1.29 ± 0.07 [mean ± SD], 11 cell lines; *8701G/10398G*, 1.25 ± 0.07 [mean ± SD], 22 cell lines; $p > 0.10$, Mann-Whitney *U* test). This result suggests that cytosolic calcium response may be enhanced in the *8701A/10398A* cybrids.

The nucRP data from the replication study using cybrid cell lines stably expressing RP confirmed that peak cytosolic calcium levels after histamine stimulation were higher in the *8701A/10398A* cybrids than in *8701G/10398G* cybrids (*8701A/10398A*, 2.56 ± 0.03 [mean ± SD], three cell lines; *8701G/10398G*, 2.26 ± 0.16 [mean ± SD], three cell lines).

Discussion

In the present study, we comprehensively searched for mtDNA polymorphisms that alter the fluorescence ratios of mtRP, and we identified two mtDNA single nucleotide

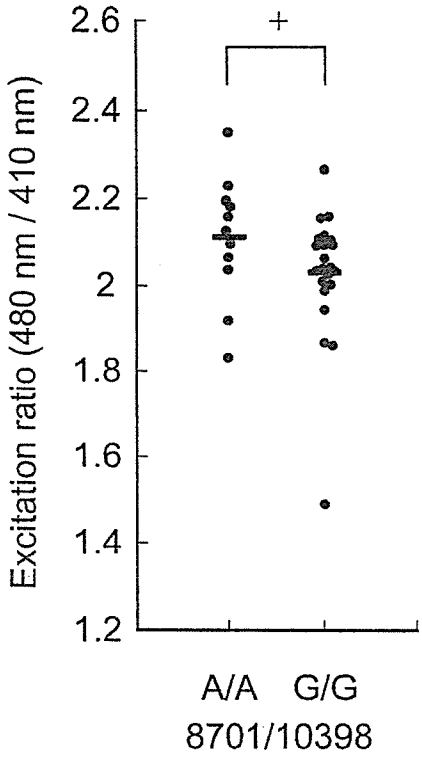

Figure 4. Peak Cytosolic Calcium Level after Histamine Stimulation in Cybrids with *8701A/10398A* and *8701G/10398G*

The values of two cybrids with *8701A/10398G* were 1.92 and 2.20. For each cybrid, data taken from 11–42 cells (average, 26 cells) were averaged. The *y* axis shows the ratio of the 525 nm fluorescence at 480 nm to that at 410 nm. Horizontal bars indicate the mean values for each type of cybrid. $+p = 0.08$ (Mann-Whitney *U* test).

DOI: 10.1371/journal.pgen.0020128.g004

polymorphisms (mtSNPs), *10398A* and *8701A*, that increase the basal fluorescence ratios of mtRP.

In the *10398A/G* mtSNP, threonine is substituted by alanine at the C terminus of ND3, a subunit of complex I (NADH: ubiquinone oxidoreductase) [10]. In the *8701A/G* mtSNP, there is an amino acid substitution from threonine to alanine at ATPase6, the F0 subunit 6 of complex V (ATP synthase) [10]. Complex I generates a proton gradient across mitochondrial inner membrane by exporting protons, whereas ATP synthase produces ATP by using this proton gradient. The proton gradient is also the driving force of calcium uptake by mitochondria. Therefore, both polymorphisms can affect the proton gradient across mitochondrial inner membrane and calcium levels.

During the course of our study, it was reported that the fluorescence ratio of RP is dependent not only on calcium levels but also on pH at the higher pH ranges in mitochondrial matrix [32,33]. Thus, we measured basal mitochondrial matrix pH in cybrids with *8701A/10398A* and *8701G/10398G*. Basal mitochondrial matrix pH was significantly lower in cybrids with *8701A/10398A* than in those with *8701G/10398G*. Alteration in mitochondrial pH has also been hypothesized to modulate ATP production, apoptosis, and the opening of the mitochondrial membrane permeability transition pore [44]. Transport of protons is coupled with electron transport by a respiratory chain consisting of complexes I, III, and IV. As described above, the mtDNA 10398 polymorphism affects the amino acid composition in a subunit of complex I. When the activity of complex I in the electron-transport chain was measured using citrate synthase activity as a reference [45], the activity of *8701A/10398A* cybrids tended to be lower than that of *8701G/10398G* cybrids (*8701A/10398A*, 5.77 ± 1.41 [mean ± SD], four cell lines; *8701G/10398G*, 7.58 ± 1.27 [mean ± SD], four cell lines; $p = 0.10$, *t* test). This finding supports the above-mentioned difference in mitochondrial matrix pH.

The difference in basal mitochondrial matrix pH could not contribute to the initial finding of higher mtRP fluorescence ratio in the cybrids with *8701A/10398A* because lower pH could only decrease the mtRP fluorescence rate, not increase it. Therefore, the most probable interpretation for the difference in basal mtRP fluorescence ratio is higher mitochondrial calcium levels in cybrids carrying *8701A/10398A*. In addition, the calcium responses to histamine stimulation tended to be higher in the cytosol of *8701A/10398A* cybrids than *8701G/10398G* cybrids, both in the initial experiment and the replication study using cybrid cell lines stably expressing RP. These findings suggest that alterations in mitochondrial function cause the enhanced cytosolic calcium response and higher basal mitochondrial calcium levels in cybrids with *8701A/10398A*.

Mitochondria have several calcium transport mechanisms. Calcium uptake is attributable to a mitochondrial calcium uniporter in inner mitochondrial membrane. Calcium efflux from mitochondria is mediated by the Na^+/Ca^{2+} exchanger and the H^+/Ca^{2+} antiporter. The opening of the membrane permeability transition pore also allows efflux of calcium from mitochondria. Clarification of mitochondrial calcium transport systems at the molecular level would facilitate the understanding of biochemical mechanism of how the 10398 polymorphism alters mitochondrial calcium dynamics. Further study is needed to reveal how these two mtSNPs alter mitochondrial matrix pH and calcium levels.

Among the two polymorphisms we found to have functional significance, *10398A/G* has previously been associated with human health and diseases. The *10398G* polymorphism is reportedly associated with a reduced risk of Parkinson disease [19], whereas *10398A* was reported to increase the risk of Alzheimer disease in men [17], invasive breast cancer in African-American women [24], and prostate cancer in African-American men [25]. In addition, *10398A* is reportedly associated with an increased risk of bipolar disorder [22,23,46]. According to the mtSNP database (http://www.gen-b.or.jp/mtsnp/index_e.html), most Europeans have *8701A*, but it is polymorphic in the Japanese population. In contrast, *10398A* is polymorphic both in Europeans and Japanese. The *10398A/G* characterizes the European haplogroup I, J, and K [17], and Asian-specific super haplogroup M [47]. Thus, the present findings can be translated that Asian-specific super haplogroup M is associated with different mitochondrial pH and calcium from other Asian-specific haplogroups.

The frequency of *10398A* is much smaller in the Japanese population (approximately 29% in the mtSNP database) compared with Europeans (approximately 74% in the mtSNP database). The average life expectancy in Japan is the highest in the world, and its biological basis is not yet well understood. Tanaka et al. sequenced the whole mtDNA sequence in

11 Japanese centenarians and reported that a subset of haplogroup M characterized by several mtDNA polymorphisms is more frequently seen in centenarians [48]. Among these polymorphisms, they have mainly focused on the *5178A* polymorphism that characterizes haplogroup D in super haplogroup M. The *5178C/A* is associated with several common diseases such as Parkinson disease [28], atherosclerosis in patients with diabetes mellitus [49], and myocardial infarction [50]. A recent study, however, suggested that association of *5178A* with longevity is ethnicity dependent [51]. Therefore, it might be possible that these apparent effects of *5178C/A* in the Japanese population may be mediated by the other linked polymorphisms that cause functional change. Although *5178A* did not affect the fluorescence ratio of mtRP in this study, most subjects with *5178A* have *10398G*. Thus, it could be possible that *10398G* mediates these apparent associations of *5178C/A* with complex diseases and longevity. In fact, based on the mtSNP database, *10398G* was significantly more frequently seen in centenarians (76 of 96 [79%]) compared with young Japanese (129 of 192 [67%]; $p = 0.03$). A recent study by Niemi et al. also suggested that *10398G* affects longevity [52].

To date, there has been no study on the association of *8701A/G* with health and disease, and information on *8701A/G* is limited. Most of the above-noted associations with the 5178 polymorphism observed in the Japanese population could also be mediated by 8701, since it is closely linked with 10398 and 5178. In fact, *8701G* is also more frequency seen in centenarians (68 of 96 [71%]) compared with young Japanese (111 of 192 [58%]; $p = 0.03$).

It was difficult to assess the functional effects of these two mtSNPs separately, because there were only two subjects carrying *8701A/10398G* in our sample set. Although it is still an open question whether or not *8701A/G* causes some functional change, at least *10398A/G* seems to have some functional significance. The tendency of altered complex I activity between the *8701A/10398A* and *8701G/10398G* cybrids suggest that the observed difference between *8701A/10398A* and *8701G/10398G* is mediated at least partly by the functional alteration of complex I by *10398A/G*.

Because there was considerable overlap, including an outlier, with regard to the basal mtRP fluorescence between *8701A/10398A* and *8701G/10398G*, there might be a concern that the observed difference may be caused by those outliers. Thus, we applied the Smirnov-Grubbs test for the detection of outliers. One cell line, having the lowest value in the *8701G/10398G* group, was found to be an outlier ($T = 3.17$; $p < 0.05$). Even after this cell line was omitted, basal mtRP fluorescence ratios in cybrids with *8701A/10398A* were significantly higher than those with *8701G/10398G* (*8701A/10398A*, 1.67 ± 0.09 [mean ± SD], $n = 11$; *8701G/10398G*, 1.60 ± 0.09 [mean ± SD], $n = 21$; $p < 0.05$, Mann-Whitney U test). Thus, the observed difference was not due to the effect of the outlier. One might suspect that observed variation of basal mtRP fluorescence ratios might not be caused by mtDNA sequence variation but resulted from an experimental variation. However, the interassay variance within one cybrid cell line having the same mtDNA sequence was significantly smaller than the variation among cybrid cell lines having different mtDNA sequences. This indicates that observed variation of mtRP fluorescence ratios among cybrid cell lines were not caused by experimental variation but caused by the difference of mtDNA sequence.

There might be the other concern that the present finding is somehow affected by the process of subcloning, and such a finding cannot be generalized. However, in our replication study using independently established cybrid cell lines, it was confirmed that the observed finding was not specific to this particular subcloned cybrids, but was actually caused by differences of mtDNA sequences.

In summary, we identified two mtSNPs that were suggested to alter mitochondrial matrix pH and intracellular calcium dynamics. To our knowledge, this is the first report of mtDNA polymorphisms affecting these intracellular functions. Among the two mtSNPs examined, the *10398A/G* polymorphism was previously reported to be associated with Parkinson disease, Alzheimer disease, some kinds of cancer, bipolar disorder, and longevity. A drug that affects mitochondrial matrix pH or calcium levels might be a promising strategy for health and disease.

Materials and Methods

Subjects. Cybrids were generated from platelets derived from 35 volunteers, 17 patients with bipolar disorder (mean age, 48 years; 9 men and 8 women) and 18 healthy controls (mean age, 48 years; 10 men and 8 women). All were Japanese. Patients with bipolar disorder were included in this study because these blood samples were collected as a part of a project to study the genetics of bipolar disorder. None of the experimental parameters reported in this paper showed a significant difference between patients and controls. Diagnoses were made by the consensus of two senior psychiatrists using the DSM-IV criteria. Written informed consent was obtained from all volunteers. The Ethics Committees of the RIKEN Brain Science Institute and other participating institutes approved the study. For the replication study using cybrid cell lines stably expressing RP, we selected cybrids from three subjects with *8701A/10398A* mtDNA (mean age, 48 years; 1 man and 2 women) and three subjects with *8701G/10398G* mtDNA (mean age, 51 years; 1 man and 2 women). Cybrids for replication studies using independently established cybrid cell lines and measurements of mitochondrial matrix pH were generated using platelets from four *8701A/10398A* subjects (mean age, 52 years; 2 men and 2 women) and four *8701G/10398G* subjects (mean age, 56 years; 2 men and 2 women). Cybrids for replication studies and the measurement of mitochondrial matrix pH were derived from healthy controls. Although these cell lines have several mtDNA polymorphisms in addition to 8701 and 10398, they were carefully selected so that they have minimum difference in other positions of mtDNA.

Generation of the 143B.TK$^-$ $\rho^0$206 cell line stably carrying calcium-sensitive probes. The 143B.TK$^-$ $\rho^0$206 cell line derived from the osteosarcoma cell line (143B.TK$^-$) was established by Attardi and King [30]. The 143B.TK$^-$ $\rho^0$206 cells were grown in DMEM (Invitrogen, Carlsbad, California, United States), supplemented with 10% FBS, 50 U penicillin, 50 μg/ml streptomycin, and 50 μg/ml uridine. The cells were grown on dishes 35 mm in diameter to 50% confluence. The cells were cotransfected with Lipofect AMINE PLUS (Invitrogen) with *ratiometric Pericam-nuc* (0.25 μg DNA/dish) and *ratiometric coxIV-Pericam* (0.75 μg DNA/dish) cDNAs. After 2 d, these cells were replated onto coverslips 14 mm in diameter and allowed to grow to 2.5% confluence with selection medium, supplemented with 10% FBS, 1,000 μg/ml geneticin (Invitrogen), and 50 μg/ml uridine. After 2 wk, a single colony with fluorescence in nuclei and mitochondria was picked up under a fluorescent microscope. mtDNA-specific PCR and Southern blot analysis were used to confirm that the cells lacked mtDNA. The cell lines were replated onto coverslips and stimulated by histamine (Sigma-Aldrich, Saint Louis, Missouri, United States) as described below. One of the ten cell lines had a reproducible calcium response without spontaneous calcium oscillation. This line was selected for further examination.

Generation of cybrid cell lines. Peripheral blood was drawn into a 10 ml Vactainer tube containing 1.5 ml acid citrate dextrose (BD Biosciences, Palo Alto, California, United States). Platelets were separated by centrifugation at a speed of 1,200 rpm for 20 min. The

143B.TK$^-$ $\rho^0$206 cells that had been stably expressing RPs were fused with platelets from individuals using a polyethylene glycol solution [53]. After 3 d of fusion, the medium was replaced by a selection medium without uridine. After 2 wk, surviving cells were collected. The integration of mtDNA was verified by Southern blot analysis as previously described with some modifications [54]. Cybrids for the replication study using independently established cybrid cell lines and measurements of mitochondrial matrix pH were generated by fusing the native 143B.TK$^-$ $\rho^0$206 cells and platelets from individuals as described above.

Measurements of fluorescence ratios of RP. Cybrids in modified Krebs R buffer (125 mM NaCl, 5 mM KCl, 5.5 mM glucose, 20 mM HEPES, and 1 mM $MgCl_2$ [pH 7.4]) were imaged at room temperature on an Olympus IX-70 (Olympus, Tokyo, Japan) with a CoolSNAPHQ CCD camera (Roper Scientific, Tucson, Arizona, United States) controlled by Universal Imaging Meta series 4.5/4.6 (Universal Imaging, Media, Pennsylvania, United States). Dual-excitation imaging with RP used two excitation filters (480DF10 and 410DF10), alternated by a Lambda 10–2 filter exchanger (Sutter Instruments, Novato, California, United States), a 505DRLP-XR dichroic mirror, and a 525AF45 emission filter. The cybrids were stimulated by bath-application of 10 μM histamine applied to the coverslip. The ratio of the 525 nm fluorescence at 480 nm to that at 410 nm was used for further analysis. The regions of interest for measuring calcium response in each cell were the mitochondria and nucleus.

For each cell line, 11–42 cells were measured. At first, the basal fluorescence ratios of mtRP obtained from each cell were used for statistical analysis by one-way analysis of variance. Using one-way analysis of variance ($df = 34$), we tested whether or not the variation among 35 cybrid cell lines having different mtDNA was larger than the variation within one cell line. Then, the 11–42 data points in each cell line were averaged to calculate the representative value for each cell line.

The coefficient of variation in fluorescence ratio of mtRP in each cell line was 12.2% ± 3.2% (mean ± SD in 35 cybrids).

For the replication study using eight independently established cybrid cell lines (four with *8701A/10398A* mtDNA and four with *8701G/10398G* mtDNA), cybrids were transiently transfected with *ratiometric coxIV-Pericam* (1 μg DNA/dish) cDNA using Lipofect AMINE PLUS. After 2 d, measurements were performed in these cell lines. Different from the case in the cells stably expressing RP, there is no assurance that the expression level of RP is constant across cells in this experiment, which may potentially affect the stability of fluorescence ratio. To avoid the effect of variability of expression levels of RP among cells, we performed in vivo calibration for each cell. To exactly estimate calcium levels, we applied histamine stimulation to the cells, and only those responded to histamine were further analyzed. Cells responded to calcium could be found in three of four cell lines for each group. Cells were stimulated by 10 μM histamine, and calibration was performed using calibration buffers. Calcium-free buffer consisted of modified Krebs R buffer with 10 μM ionomycin (Calbiochem, San Diego, California, United States), 50 μM BAPTA-AM (Dojindo Laboratories, Kumamoto, Japan), and 10 mM EGTA (Dojindo Laboratories). Calcium saturation buffer was made of modified Krebs R buffer with 10 μM ionomycin and 10 mM $CaCl_2$. $[Ca^{2+}]$ measured by in situ calibration was calculated by the equation $[Ca^{2+}] = K'_d [(R - R_{min}) / (R_{max} - R)]^{(1/n)}$, where K'_d is the apparent dissociation constant corresponding to the calcium concentration and n is the Hill coefficient [55]. Because K'_d and n are constants but K'_d of RP in mitochondria is not known, we simply used the value of $(R - R_{min}) / (R_{max} - R)$ for the assessment of mitochondrial calcium level. The condition for imaging is basically similar to those described above.

Analysis of entire sequences of mtDNA. Total DNA was extracted from each cybrid using standard protocols. The entire mtDNA was sequenced as described [56]. A computer program, Sequencher version 4.1.1 (Gene Codes, Ann Arbor, Michigan, United States), was used to indicate possible SNP loci. For verification, visual inspection of each candidate SNP was carried out. At least two overlapping DNA templates amplified with different primer pairs were used for identification of each SNP. mtSNPs were identified by comparison with the revised Cambridge sequence (GI1944628) reported by Andrews et al. [37]. For all polymorphisms that resulted in changed amino acid sequence or those within rRNA or tRNA regions, averaged fluorescence ratios of mtRP were compared between genotypes by Mann-Whitney *U* test. This analysis was performed only when three or more cybrids had the same polymorphism. For statistical analysis, Mann-Whitney *U* tests were applied using SPSS software (SPSS, Tokyo, Japan).

Construction of pH indicator for measurements of mitochondrial matrix pH. *GFP* variants were prepared as described [57]. As a template, the original *GFP* mutation was employed. This template incorporates the mutation [58,58]. Mutations were verified by sequencing the entire gene. The *pH-GFP* [39] with polyhistidine tag at the N terminus was expressed in *Escherichia coli* JM109 (DE3) (Promega, Madison, Wisconsin, United States), purified, and spectroscopically characterized as described [55]. The gene for *mt pH-GFP* was amplified by PCR using the *GFP* variants as a template, with a forward primer containing *complex IV* mitochondrial target sequences and an MluI site, and a reverse primer containing an EcoRV site. The gene for *mt DsRed* was amplified by PCR using p*DsRed1-1 Mito* as a template with a forward primer containing a NotI site and a reverse primer containing a SalI site. The restricted *mt pH-GFP* product was subcloned in-frame into multiple cloning site I, and *mt DsRed* was subcloned into multiple cloning site II of the pBI bidirectional Tet vector (Clontech Laboratories, Mountain View, California, United States).

Transient expression of pH indicator in cybrid cell lines using the Tet system. To ensure the same expression levels of two genes, *mt pH-GFP* and *mt DsRed*, the bidirectional Tet expression vector was used in Tet-Off Gene expression systems [40,41]. The pBI bidirectional Tet expression vector contains a "bidirectional" promoter composed of a tetracycline-response element flanked by two minimal cytomegalovirus promoters in opposite orientations [42]. To induce these two genes, the other vector expressing the tetracycline-controlled transactivator under the cytomegalovirus promoter control was cotransfected.

Cybrids were grown in DMEM (Sigma-Aldrich) supplemented with 10% Tet system-approved FBS (Clontech), 100 U penicillin, and 100 μg/ml streptomycin. The cells were grown on dishes 35 mm in diameter to about 80% confluence. The cells were cotransfected with Tet-Off vector (Clontech) and pBI-*(mt pH-GFP)*-*(mt DsRed)* (total 1 μg DNA/dish) using Lipofect AMINE PLUS (Invitrogen). After 2 d, mitochondrial matrix pH was measured in these cells.

Mitochondrial matrix pH measurements and in vivo calibration. Cybrids in modified Krebs R buffer were imaged at room temperature. The imaging system is described above. Imaging with mt pH-GFP/DsRed used two excitation filters (480DF10 and S565/25), a dichroic mirror for GFP/DsRed, and emission filters (525AF45 and S620/60).

It was confirmed that the fluorescence ratio (525 nm/620 nm) decreased after the treatment with FCCP (Sigma-Aldrich), suggesting that this set of fluorescent indicators is sensitive to the mitochondrial matrix pH.

For in situ calibration, cybrids were perfused with the following pH titration buffer (125 mM KCl, 20 mM NaCl, 0.5mM $CaCl_2$, 0.5 mM $MgCl_2$, and 25 mM pH buffer [MOPS was used for pH 7.0, HEPES for pH 7.5 and 8.0, and glycylglycine for pH 8.5]) [59]. All calibration experiments were carried out in the presence of 10 μM nigericin and 10 μM monensin (Sigma-Aldrich). After baseline measurements were recorded for several minutes, calibration was performed in vivo. The fluorescence ratio of 525 nm emission at 480 nm excitation to 620 nm emission at 565 nm excitation reflected the dynamics of mitochondrial matrix pH. Mitochondrial matrix pH was calculated by plotting the calibration curve of each cell.

Supporting Information

Figure S1. Effects of *8701A/10398A* and *8701G/10398G* on Basal Mitochondrial Calcium Levels Measured by mtRP

The *y* axis shows the basal mitochondrial calcium levels indicated by the value of $(R - R_{min}) / (R_{max} - R)$ measured by mtRP. In situ calibration for $[Ca^{2+}]$ uses the equation $[Ca^{2+}] = K'_d [(R - R_{min}) / (R_{max} - R)]^{(1/n)}$. R is the basal ratio of the 525 nm fluorescence at 480 nm to that at 410 nm. R_{min} is the ratio at free calcium. R_{max} is the ratio at saturating calcium. K'_d is the apparent dissociation constant. n is the Hill coefficient. Bars indicate the standard error of mean for each cybrid cell line.

Found at DOI: 10.1371/journal.pgen.0020128.sg001 (120 KB PDF).

Table S1. mtDNA Polymorphisms in Eight Cybrids

Found at DOI: 10.1371/journal.pgen.0020128.st001 (97 KB XLS).

Acknowledgments

We sincerely thank the members of the Laboratory for Cell Function and Dynamics at the RIKEN Brain Science Institute. We thank the

members of the Research Resource Center at the RIKEN Brain Science Institute, especially Mr. Miyazaki, for technical assistance. We thank Ms. Bonnie Lee La Madeleine and Dr. S. Takeda, and Dr. T. Yoshida for valuable suggestions on the manuscript.

Author contributions. TK conceived and designed the experiments. AK and KM performed the experiments. AK and TK analyzed the data. AK, KM, TN, SS, MT, MY, NK, AM, and TK contributed reagents/materials/analysis tools. AK and TK wrote the paper.

Funding. This work was supported by an Independent Investigator Award from the National Alliance for Research on Schizophrenia and Depression (NARSAD) to T.K., a grant from the Japanese Ministry of Health, Labour and Welfare, and a grant from Japanese Ministry of Education, Culture, Sports, Science and Technology.

Competing interests. The authors have declared that no competing interests exist.

References

1. Hansford RG, Zorov D (1998) Role of mitochondrial calcium transport in the control of substrate oxidation. Mol Cell Biochem 184: 359–369.
2. Cortassa S, Aon MA, Marban E, Winslow RL, O'Rourke B (2003) An integrated model of cardiac mitochondrial energy metabolism and calcium dynamics. Biophys J 84: 2734–2755.
3. Demaurex N, Distelhorst C (2003) Cell biology. Apoptosis—The calcium connection. Science 300: 65–67.
4. Hajnoczky G, Davies E, Madesh M (2003) Calcium signaling and apoptosis. Biochem Biophys Res Commun 304: 445–454.
5. Rizzuto R, Pinton P, Ferrari D, Chami M, Szabadkai G, et al. (2003) Calcium and apoptosis: Facts and hypotheses. Oncogene 22: 8619–8627.
6. Kaftan EJ, Xu T, Abercrombie RF, Hille B (2000) Mitochondria shape hormonally induced cytoplasmic calcium oscillations and modulate exocytosis. J Biol Chem 275: 25465–25470.
7. Medler K, Gleason EL (2002) Mitochondrial Ca(2+) buffering regulates synaptic transmission between retinal amacrine cells. J Neurophysiol 87: 1426–1439.
8. Weeber EJ, Levy M, Sampson MJ, Anflous K, Armstrong DL, et al. (2002) The role of mitochondrial porins and the permeability transition pore in learning and synaptic plasticity. J Biol Chem 277: 18891–18897.
9. Li Z, Okamoto K, Hayashi Y, Sheng M (2004) The importance of dendritic mitochondria in the morphogenesis and plasticity of spines and synapses. Cell 119: 873–887.
10. Anderson S, Bankier AT, Barrell BG, de Bruijn MH, Coulson AR, et al. (1981) Sequence and organization of the human mitochondrial genome. Nature 290: 457–465.
11. Goto Y, Nonaka I, Horai S (1990) A mutation in the tRNA(Leu)(UUR) gene associated with the MELAS subgroup of mitochondrial encephalomyopathies. Nature 348: 651–653.
12. Kobayashi Y, Momoi MY, Tominaga K, Momoi T, Nihei K, et al. (1990) A point mutation in the mitochondrial tRNA(Leu)(UUR) gene in MELAS (mitochondrial myopathy, encephalopathy, lactic acidosis and stroke-like episodes). Biochem Biophys Res Commun 173: 816–822.
13. Hess JF, Parisi MA, Bennett JL, Clayton DA (1991) Impairment of mitochondrial transcription termination by a point mutation associated with the MELAS subgroup of mitochondrial encephalomyopathies. Nature 351: 236–239.
14. Smeitink J, van den Heuvel L, DiMauro S (2001) The genetics and pathology of oxidative phosphorylation. Nat Rev Genet 2: 342–352.
15. Poulton J, Luan J, Macaulay V, Hennings S, Mitchell J, et al. (2002) Type 2 diabetes is associated with a common mitochondrial variant: Evidence from a population-based case-control study. Hum Mol Genet 11: 1581–1583.
16. Hutchin T, Cortopassi G (1995) A mitochondrial DNA clone is associated with increased risk for Alzheimer disease. Proc Natl Acad Sci U S A 92: 6892–6895.
17. van der Walt JM, Dementieva YA, Martin ER, Scott WK, Nicodemus KK, et al. (2004) Analysis of European mitochondrial haplogroups with Alzheimer disease risk. Neurosci Lett 365: 28–32.
18. Shoffner JM, Brown MD, Torroni A, Lott MT, Cabell MF, et al. (1993) Mitochondrial DNA variants observed in Alzheimer disease and Parkinson disease patients. Genomics 17: 171–184.
19. van der Walt JM, Nicodemus KK, Martin ER, Scott WK, Nance MA, et al. (2003) Mitochondrial polymorphisms significantly reduce the risk of Parkinson disease. Am J Hum Genet 72: 804–811.
20. Huerta C, Castro MG, Coto E, Blazquez M, Ribacoba R, et al. (2005) Mitochondrial DNA polymorphisms and risk of Parkinson's disease in Spanish population. J Neurol Sci 236: 49–54.
21. Ghezzi D, Marelli C, Achilli A, Goldwurm S, Pezzoli G, et al. (2005) Mitochondrial DNA haplogroup K is associated with a lower risk of Parkinson's disease in Italians. Eur J Hum Genet 13: 748–752.
22. Kato T, Kunugi H, Nanko S, Kato N (2001) Mitochondrial DNA polymorphisms in bipolar disorder. J Affect Disord 62: 151–164.
23. McMahon FJ, Chen YS, Patel S, Kokoszka J, Brown MD, et al. (2000) Mitochondrial DNA sequence diversity in bipolar affective disorder. Am J Psychiatry 157: 1058–1064.
24. Canter JA, Kallianpur AR, Parl FF, Millikan RC (2005) Mitochondrial DNA G10398A polymorphism and invasive breast cancer in African-American women. Cancer Res 65: 8028–8033.
25. Mims MP, Hayes TG, Zheng S, Leal SM, Frolov A, et al. (2006) Mitochondrial DNA G10398A polymorphism and invasive breast cancer in African-American women. Cancer Res 66:: 1880; author reply 1880–1881.
26. Skuder P, Plomin R, McClearn GE, Smith DL, Vignetti S, et al. (1995) A polymorphism in mitochondrial DNA associated with IQ? Intelligence 21: 1–11.
27. Kato C, Umekage T, Tochigi M, Otowa T, Hibino H, et al. (2004) Mitochondrial DNA polymorphisms and extraversion. Am J Med Genet 128B: 76–79.
28. Tanaka M, Takeyasu T, Fuku N, Li-Jun G, Kurata M (2004) Mitochondrial genome single nucleotide polymorphisms and their phenotypes in the Japanese. Ann N Y Acad Sci 1011: 7–20.
29. Tanaka M, Gong J, Zhang J, Yamada Y, Borgeld HJ, et al. (2000) Mitochondrial genotype associated with longevity and its inhibitory effect on mutagenesis. Mech Ageing Dev 116: 65–76.
30. King MP, Attardi G (1989) Human cells lacking mtDNA: Repopulation with exogenous mitochondria by complementation. Science 246: 500–503.
31. Nagai T, Sawano A, Park ES, Miyawaki A (2001) Circularly permuted green fluorescent proteins engineered to sense Ca^{2+}. Proc Natl Acad Sci U S A 98: 3197–3202.
32. Filippin L, Magalhaes PJ, Di Benedetto G, Colella M, Pozzan T (2003) Stable interactions between mitochondria and endoplasmic reticulum allow rapid accumulation of calcium in a subpopulation of mitochondria. J Biol Chem 278: 39224–39234.
33. Frieden M, James D, Castelbou C, Danckaert A, Martinou JC, et al. (2004) Ca(2+) homeostasis during mitochondrial fragmentation and perinuclear clustering induced by hFis1. J Biol Chem 279: 22704–22714.
34. Llopis J, McCaffery JM, Miyawaki A, Farquhar MG, Tsien RY (1998) Measurement of cytosolic, mitochondrial, and Golgi pH in single living cells with green fluorescent proteins. Proc Natl Acad Sci U S A 95: 6803–6808.
35. Porcelli AM, Ghelli A, Zanna C, Pinton P, Rizzuto R, et al. (2005) pH difference across the outer mitochondrial membrane measured with a green fluorescent protein mutant. Biochem Biophys Res Commun 326: 799–804.
36. Brini M, Pinton P, King MP, Davidson M, Schon EA, et al. (1999) A calcium signaling defect in the pathogenesis of a mitochondrial DNA inherited oxidative phosphorylation deficiency. Nat Med 5: 951–954.
37. Andrews RM, Kubacka I, Chinnery PF, Lightowlers RN, Turnbull DM, et al. (1999) Reanalysis and revision of the Cambridge reference sequence for human mitochondrial DNA. Nat Genet 23: 147.
38. Elsliger MA, Wachter RM, Hanson GT, Kallio K, Remington SJ (1999) Structural and spectral response of green fluorescent protein variants to changes in pH. Biochemistry 38: 5296–5301.
39. Matsuyama S, Llopis J, Deveraux QL, Tsien RY, Reed JC (2000) Changes in intramitochondrial and cytosolic pH: Early events that modulate caspase activation during apoptosis. Nat Cell Biol 2: 318–325.
40. Gossen M, Bujard H (1992) Tight control of gene expression in mammalian cells by tetracycline-responsive promoters. Proc Natl Acad Sci U S A 89: 5547–5551.
41. Gossen M, Freundlieb S, Bender G, Muller G, Hillen W, et al. (1995) Transcriptional activation by tetracyclines in mammalian cells. Science 268: 1766–1769.
42. Baron U, Freundlieb S, Gossen M, Bujard H (1995) Co-regulation of two gene activities by tetracycline via a bidirectional promoter. Nucleic Acids Res 23: 3605–3606.
43. Mizuno H, Sawano A, Eli P, Hama H, Miyawaki A (2001) Red fluorescent protein from *Discosoma* as a fusion tag and a partner for fluorescence resonance energy transfer. Biochemistry 40: 2502–2510.
44. Bernardi P (1992) Modulation of the mitochondrial cyclosporin A–sensitive permeability transition pore by the proton electrochemical gradient. Evidence that the pore can be opened by membrane depolarization. J Biol Chem 267: 8834–8839.
45. Trounce IA, Kim YL, Jun AS, Wallace DC (1996) Assessment of mitochondrial oxidative phosphorylation in patient muscle biopsies, lymphoblasts, and transmitochondrial cell lines. Methods Enzymol 264: 484–509.
46. Kato T (2001) DNA polymorphisms and bipolar disorder. Am J Psychiatry 158: 1169–1170.
47. Sudoyo H, Suryadi H, Lertrit P, Pramoonjago P, Lyrawati D, et al. (2002) Asian-specific mtDNA backgrounds associated with the primary G11778A mutation of Leber's hereditary optic neuropathy. J Hum Genet 47: 594–604.
48. Tanaka M, Gong JS, Zhang J, Yoneda M, Yagi K (1998) Mitochondrial genotype associated with longevity. Lancet 351: 185–186.
49. Matsunaga H, Tanaka Y, Tanaka M, Gong JS, Zhang J, et al. (2001) Antiatherogenic mitochondrial genotype in patients with type 2 diabetes. Diabetes Care 24: 500–503.

50. Takagi K, Yamada Y, Gong JS, Sone T, Yokota M, et al. (2004) Association of a 5178C→A (Leu237Met) polymorphism in the mitochondrial DNA with a low prevalence of myocardial infarction in Japanese individuals. Atherosclerosis 175: 281–286.
51. Dato S, Passarino G, Rose G, Altomare K, Bellizzi D, et al. (2004) Association of the mitochondrial DNA haplogroup J with longevity is population specific. Eur J Hum Genet 12: 1080–1082.
52. Niemi AK, Moilanen JS, Tanaka M, Hervonen A, Hurme M, et al. (2005) A combination of three common inherited mitochondrial DNA polymorphisms promotes longevity in Finnish and Japanese subjects. Eur J Hum Genet 13: 166–170.
53. Bentlage HA, Chomyn A (1996) Immunoprecipitation of human mitochondrial translation products with peptide-specific antibodies. Methods Enzymol 264: 218–228.
54. Nishino I, Kobayashi O, Goto Y, Kurihara M, Kumagai K, et al. (1998) A new congenital muscular dystrophy with mitochondrial structural abnormalities. Muscle Nerve 21: 40–47.
55. Miyawaki A, Llopis J, Heim R, McCaffery JM, Adams JA, et al. (1997) Fluorescent indicators for Ca^{2+} based on green fluorescent proteins and calmodulin. Nature 388: 882–887.
56. Tanaka M, Hayakawa M, Ozawa T (1996) Automated sequencing of mitochondrial DNA. Methods Enzymol 264: 407–421.
57. Sawano A, Miyawaki A (2000) Directed evolution of green fluorescent protein by a new versatile PCR strategy for site-directed and semi-random mutagenesis. Nucleic Acids Res 28: E78.
58. Wachter RM, Elsliger MA, Kallio K, Hanson GT, Remington SJ (1998) Structural basis of spectral shifts in the yellow-emission variants of green fluorescent protein. Structure 6: 1267–1277.
59. Ormo M, Cubitt AB, Kallio K, Gross LA, Tsien RY, et al. (1996) Crystal structure of the *Aequorea victoria* green fluorescent protein. Science 273: 1392–1395.

害による不妊の一部にセプチン系の異常が潜んでいる可能性を探索している．セプチンをマーカーとした蛍光抗体法により，精子無力症のうち25%もの症例で輪状小体形成不全を認めたが，正常対照群では皆無であった（15および未発表）．精子の形態には著しい種差のあることが知られているが，マウスだけでなくヒトでもセプチンリングは正常な鞭毛運動の必要条件のようである．セプチンリングの有無は，ヒト精子無力症の診断・分類基準として特異性が高いだけでなく，死滅あるいは凍結保存した検体でも明確に判定できることから，治療法選択や臨床研究に有用と考えられる．輪状小体形成不全を伴う精子無力症の原因がセプチン遺伝子の変異によるものかどうかは，臨床家グループが中心となって検討を進めている．

おわりに

セプチンの生物学は酵母の遺伝学に端を発する生命科学の一分野に過ぎないが，冒頭に挙げた先人たちの洞察に違わず，がん研究との接点は増え続けている．そればかりでなく，神経系や生殖系の疾患に密接に関与することも明らかになった．セプチンの医学・生物学的重要性を示す事例は今後ますます増えると予想されるが，現時点での生化学的知見はアクチンやチューブリンとは比較にならないほど少ない．これは研究の歴史が浅いことに加えて，研究の進展を妨げるいくつかの要因によるところが大きい．例えば，均質な複合体の精製が困難なこと，脱重合条件が不明なこと，特異的阻害剤がないこと，不規則な重合性によって構造解析が困難なことなどである．謎に包まれたこのGTP結合タンパク質の重合・脱重合サイクルの詳細と，その制御機構の解明につながるブレイクスルーが待ち望まれている．

1) Hartwell, L.H. (1967) *J. Bacteriol.* 93, 1662-1670
2) Byers, B. & Goetsch, L. (1976) *J. Cell Biol.* 69, 717-721
3) Kim, H.B., Haarer, B.K., & Pringle, J.R. (1991) *J. Cell Biol.* 112, 535-544
4) Neufeld, T.P. & Rubin, G.M. (1994) *Cell* 77, 371-379
5) Field, C.M., al-Awar, O., Rosenblatt, J., Wong, M.L., Alberts, B., & Mitchison, T.J. (1996) *J. Cell Biol.* 133, 605-616
6) Frazier, J.A., Wong, M.L., Longtine, M.S., Pringle, J.R., Mann, M., Mitchison, T.J., & Field, C. (1998) *J. Cell Biol.* 143, 737-749
7) Kinoshita, M. (2006) *Curr. Opin. Cell Biol.* 18, 54-60
8) Kinoshita, M., Kumar, S., Mizoguchi, A., Ide, C., Kinoshita, A., Haraguchi, T., Hiraoka, Y., & Noda, M. (1997) *Genes Dev.* 11, 1535-1547
9) Kinoshita, M. (2003) *J. Biochem.* 134, 491-496
10) Joberty, G., Perlungher, R.R., Sheffield, P.J., Kinoshita, M., Noda, M., Haystead, T., & Macara, I.G. (2001) *Nat. Cell Biol.* 3, 861-866
11) Kinoshita, M., Field, C.M., Coughlin, M.L., Straight, A.F., & Mitchison, T.J. (2002) *Dev. Cell* 3, 791-802
12) Spiliotis, E.T., Kinoshita, M., & Nelson, W.J. (2005) *Science* 307, 1781-1785
13) Hall, P.A. & Russell, S.E. (2004) *J. Pathol.* 204, 489-505
14) Kinoshita, A., Noda, M., & Kinoshita, M. (2000) *J. Comp. Neurol.* 428, 223-239
15) Ihara, M., Kinoshita, A., Yamada, S., Tanaka, H., Tanigaki, A., Kitano, A., Goto, M., Okubo, K., Nishiyama, H., Ogawa, O., Takahashi, C., Itohara, S., Nishimune, Y., Noda, M., & Kinoshita, M. (2005) *Dev. Cell* 8, 343-352

木下 専

（京都大学大学院医学研究科 先端領域融合医学研究機構 生化学・細胞生物学グループ，
科学技術振興機構 戦略的創造研究推進事業 さきがけ）

Emerging roles for the septin family of GTP-binding proteins in mitosis and cellular morphogenesis

Makoto Kinoshita (Biochemistry and Cell Biology Unit, HMRO, Kyoto University Graduate School of Medicine, Yoshida Konoe, Sakyo, Kyoto 606-8501, Japan; PRESTO, Japan Science & Technology Agency)

今，蛍光タンパク質で何ができるか？

はじめに

GFP（緑色蛍光タンパク質，以下そのファミリー全体を総称する場合は，単に「蛍光タンパク質」と呼ぶ）がなんら補因子を必要とせず，遺伝子導入するだけで生細胞内に蛍光を造り出せることが証明され，Scienceの表紙に華々しくデビューしたのが1994年．その後10年以上の歳月が流れた．その間GFPへの変異導入や様々な動物種からの類似遺伝子のクローニングにより，可視光域をほとんど網羅する波長変異体が開発されてきた．さらに，GFPの発色団の物理化学的特性やGFPが蛍光物質であるという特性を生かした様々な技術が開発されてきた．今や，興味あるタンパク質や細胞を蛍光標識したり，調べたい遺伝子プロモーターの下流に蛍光タンパク質遺伝子をつなげて細胞

に導入し，生きた状態で遺伝子の活性化を蛍光でモニターする等々のオーソドックスな利用に留まらず，タンパク質間相互作用やタンパク質機能の発現を時間的・空間的に可視化したり，光照射によりタンパク質の機能を破壊して，その生理機能を解析することも可能になってきた．これらの多くの技術を自分の研究に生かさない手はない．そこで，本稿では蛍光タンパク質を用いて今何ができるのかを，代表的な手法を幾つか挙げて解説したい．

1. GFP 発色団の電荷状態を利用したバイオセンサー

GFP の発色団（*p*-hydroxybenzyliden imidazolinone）はフェノール環を持ち，その水酸基の電荷状態に応じて異なる波長の光を吸収する．つまり，非イオン化状態では 395 nm に，イオン化状態では 470 nm に吸収ピークが現れ，両状態間の平衡がどちらにずれるかによって，吸収スペクトルが変化する．この電荷状態は発色団とそれを取り巻く様々なアミノ酸の間の複雑な電荷相互作用によって調節されており，例えば，203 番目のスレオニンをイソロイシンに置換すると非イオン化状態へ平衡がシフトするため，395 nm の吸収が優位になり（Sapphire），65 番目のセリンをスレオニンに置換するとイオン化状態へ平衡がシフトし，470 nm の吸収が優位になる（EGFP）．

タンパク質の構造変化やタンパク質間相互作用を発色団の電荷状態の変化に結びつけることができるならば，GFP の吸収スペクトルの変化を観察することによって，タンパク質の構造変化やタンパク質間相互作用を測定できるかもしれない．この発想に基づき，Baird らは Ca^{2+} 指示薬 camgaroo を開発した[1]．camgaroo は GFP の黄色変異体（YFP）の 144 番目と 145 番目のアミノ酸の間に Ca^{2+} 結合タンパク質である calmodulin（CaM）を挿入したキメラタンパク質で，CaM の Ca^{2+} 結合に伴う立体構造変化により発色団近傍の電荷相互作用が変化し，その結果 Ca^{2+} 有無での蛍光強度が 7 倍変化する．

一方，筆者らは YFP の円順列変異体（cpYFP）を用いることにより，Ca^{2+} 指示薬 pericam を開発した[2]．円順列変異とはおおもとのタンパク質の内部に新たな N 末端と C 末端を設定し，もとの C 末端と N 末端を適当なアミノ酸配列で連結する変異である．pericam は 145 番目のアミノ酸を新たな N 末端とする cp145YFP の N 末端と C 末端に，M13 ペプチドと CaM を連結している．M13 と CaM の Ca^{2+} 依存的な相互作用に伴う立体構造変化を利用して，発色団の電荷状態を変化させることを原理とする．蛍光強度が Ca^{2+} の結合により 8 倍増加する flash-pericam，逆に 7 倍減少する inverse-pericam，励起スペクトルが変化する ratiometric-pericam の 3 種類が開発されている．最近では，円順列変異蛍光タンパク質を用いたタンパク質リン酸化のバイオセンサーも作成されており[3]，本手法による様々なバイオセンサーの登場を期待したい．

GFP 発色団の周辺環境は GFP 自身の二量体化によっても影響を受けるらしい．De Angelis らは GFP 発色団の電荷状態が GFP 同士の二量体化によって影響を受ける結果，395 nm と 475 nm の吸収強度比が変化することを発見し，この性質を利用してタンパク質間相互作用を可視化する PRIM（proximity imaging）法を開発した[4]．この方法を用いて，免疫抑制剤である FK506 に依存した FKBP のホモダイマー化が生きた細胞内で観察されているが，応用例が乏しい．

2. 分割 GFP によるタンパク質間相互作用の可視化

Hu らは GFP を N 末端側と C 末端側の二つの断片に分けて発現させると，何れの断片も蛍光性を持たないが，それぞれの断片に相互作用するタンパク質を繋げると，タンパク質間相互作用を介して GFP が再構成され，蛍光発光することを見出した[5]．BiFC（bimolecular fluorescence complementation）と呼ばれる本方法により，bZIP タンパク質ファミリーと Rel タンパク質ファミリー間の相互作用が培養細胞を用いて観察されている．さらに彼らは GFP 波長変異体（青，シアン，緑，黄）の N 末端側，C 末端側断片を様々に組み合わせることによって，スペクトルが異なる 7 種類の蛍光タンパク質ができることを突き止め，多種類のタンパク質間相互作用を一つの細胞内で観察する方法も開発している[6]．

BiFC 法はタンパク質間相互作用を可視化する方法だけでなく，特異的な組織を標識する方法としても注目されている．通常，ある組織を蛍光タンパク質で標識する場合，その組織に特異的な遺伝子プロモーターの制御下で蛍光タンパク質を発現させる．しかしながら，全ての組織に特異的な遺伝子プロモーターが見出されているわけではない．そこで Zhang らは組織特異性が異なる二つの遺伝子プロモーターを利用し，それぞれの活性がオーバーラップする領域に蛍光タンパク質を発現させることができないかと考え，BiFC 法を応用した．mec-3 プロモーターに N 末端側 GFP を，egl-44 プロモーターに C 末端側 GFP を連結して線虫に遺伝子導入することで，たった二つの FLP 神経だけを蛍光標識することに成功している[7]．

BiFCのようにGFPのN末端側，C末端側断片を“非共有結合的”に複合体形成させるのではなく，“共有結合的”に連結させる方法もある．Ozawaらはタンパク質スプライシング活性を持つ酵素を用いて，分割GFPを共有結合的に連結する方法を開発し[9]，その一つの応用例として，細胞内小器官に発現する新規遺伝子を迅速に解析する方法（RING：rapid identification of novel genes）を開発した[9]．RING法はGFPのN末端側，C末端側断片のそれぞれに，タンパク質スプライシング酵素DnaEのN末端側，C末端側断片をフュージョンさせ（それぞれEGFPn-DnaEn，DnaEc-EGFPc），EGFPn-DnaEncDNAライブラリーを，DnaEc-EGFPcに細胞内小器官移行配列をフュージョンした遺伝子を作成し細胞に導入する．cDNA内に目的の細胞内小器官へ移行するタンパク質がコードされていれば，その小器官内でGFPが再構成されて蛍光性になるので，FACSで蛍光性細胞を回収後，cDNAの配列を解析すればどのような遺伝子が発現していたかが判明する．この方法を用いて，Ozawaらはミトコンドリアに発現する新規タンパク質を見出すことに成功した．

3. FRETを利用したバイオセンサー

FRET（Förster resonance energy transfer）とはドナー（エネルギー供与体）の発光スペクトルとアクセプター（エネルギー受容体）の吸収スペクトルに重なりがあり，励起状態にあるドナーの近傍に，ある相対的な位置関係を保ってアクセプターが存在すると，“無輻射的”にドナーの励起エネルギーがアクセプターに移動し，アクセプターが励起される現象である．この現象を利用して，タンパク質間相互作用やタンパク質立体構造変化をイメージングすることが可能である．そのさきがけとなったのはMiyawakiらが開発したCa^{2+}センサーのcameleonである[10]．以来，非常に多くの応用例が報告されてきたが，一つの問題点として，シグナル変化量（ダイナミックレンジ）が小さいという問題があった．しかしながら最近，筆者らによってダイナミックレンジを大きくする方法が開発され，高性能なバイオセンサー開発へ応用されている[11~13]．

さて，FRETという単語自体はすっかり人口に膾炙した感があるが，その現象はしっかり理解されていないと感じることが多々ある．例えば，FRETが「ドナーから一旦放出された蛍光がアクセプターに吸収される」という誤解である．この現象は“蛍光の再吸収”であり，FRETがおおよそ10 nm以内の分子間距離で起こるのに対し，分子間距離に依存しない現象である．厄介なのは“蛍光の再吸収”の場合もドナーの蛍光が減って，アクセプターの蛍光が増えるので，一見FRETが起きているように見えることである．従って，FRETで分子間相互作用を解析しようとしているにもかかわらず，実は“蛍光の再吸収”を観察してしまい，“分子間相互作用が起こっている”と誤認してしまう場合があるので注意しなければならない．FRETが起きているのかどうかを確認する方法としてアクセプターを褪色させてドナーの蛍光強度増加を観察するアクセプター褪色法がしばしば用いられるが，本方法でもFRETと“蛍光の再吸収”を区別することができないことを銘記されたい．細胞膜や核膜など蛍光分子の実効濃度が高く，かつ分子の配向が揃いやすい領域でのタンパク質相互作用をFRETで観察する場合は，蛍光の再吸収が起きやすいため，アクセプター褪色法以外の幾つかの方法で検証することをお勧めする．ドナーの蛍光寿命の増減によりFRETを観察する蛍光寿命イメージング法（FLIM）はFRETと“蛍光の再吸収”を区別できる最良の顕微法であるため，FLIMの利用も一考されたい．但し，誰もが簡便にFLIM観察できる顕微システムがリリースされていないのが現状ではあるが．

4. 蛍光タンパク質を用いて標的分子を壊す

蛍光分子に励起光を与えると程度の大小はあるが，活性酸素が産生される．蛍光分子が強い励起光で褪色してしまうのは，自らが産生した活性酸素によって酸化され不可逆的に発色団の構造が変化してしまうからである．ライブイメージングでは禁忌であるこの現象を逆用すれば，光照射依存的に微小領域に存在する分子を任意の時間に破壊することが可能となる．いわゆるCALI（chromophore-assisted light inactivation）法と呼ばれるこの技術は専らfluoresceinなどの低分子蛍光化合物を用いて行なわれてきたが，最近になって蛍光タンパク質でも可能であることが分かってきた．蛍光タンパク質は発色団が完全にタンパク質の中に埋没しているため，産生された活性酸素はタンパク質内部で反応してしまい，外に出てこない．蛍光タンパク質が丸裸の低分子蛍光化合物ほど光毒性を示さないのはそのためである．ところが，2光子励起をした場合には効果的に活性酸素が蛍光タンパク質外に拡散し，近傍のタンパク質を破壊できることがTanabeらによって示され，MP-CALI（multiphoton excitation-evoked CALI）と命名された[14]．本方法は遺伝子ノックアウトやsiRNA法ではなし得ない，細胞内の局所領域に存在するタンパク質を任意

の時間に破壊できる方法として極めて有用な技術であるが，非常に高価な2光子顕微鏡を用いなければならないという弱点を持っていた．そんな折，通常の水銀光源でもCALIが可能な蛍光タンパク質（KillerRed）をBulinaらが開発することに成功した[15]．KillerRedをミトコンドリアマトリクスに発現させて，光照射することにより，ミトコンドリアを破壊し，アポトーシスを誘導したり，PHドメインタンパク質にKillerRedを繋げて細胞に発現させると細胞膜に局在するが，光照射依存的にPHドメインが破壊され，細胞膜から遊離する様子が観察されている．但し，KillerRedは二量体を形成するため，如何なるタンパク質にも応用できるわけではないが，早晩，単量体のものが開発されるのは先ず間違いないであろう．そうなれば蛍光タンパク質を用いて任意の時間・空間で標的分子破壊を行い，より厳密に目的タンパク質の時空間的機能を解析することができるようになるに違いない．

おわりに

多くのタンパク質を掻き集めて，試験管の中で反応させた結果から，生きた細胞内における反応を類推する，いわゆる生化学的手法は，細胞内のタンパク質間相互作用やタンパク質機能を直接可視化するリアルタイムイメージング法と対比される場合が多いが，これらの解析方法は相補的なものであり，どちらが良い悪いという次元のものではない．それぞれの利点・欠点を理解しつつ自身の研究に取り入れることにより，より包括的な生命現象の理解に迫れる

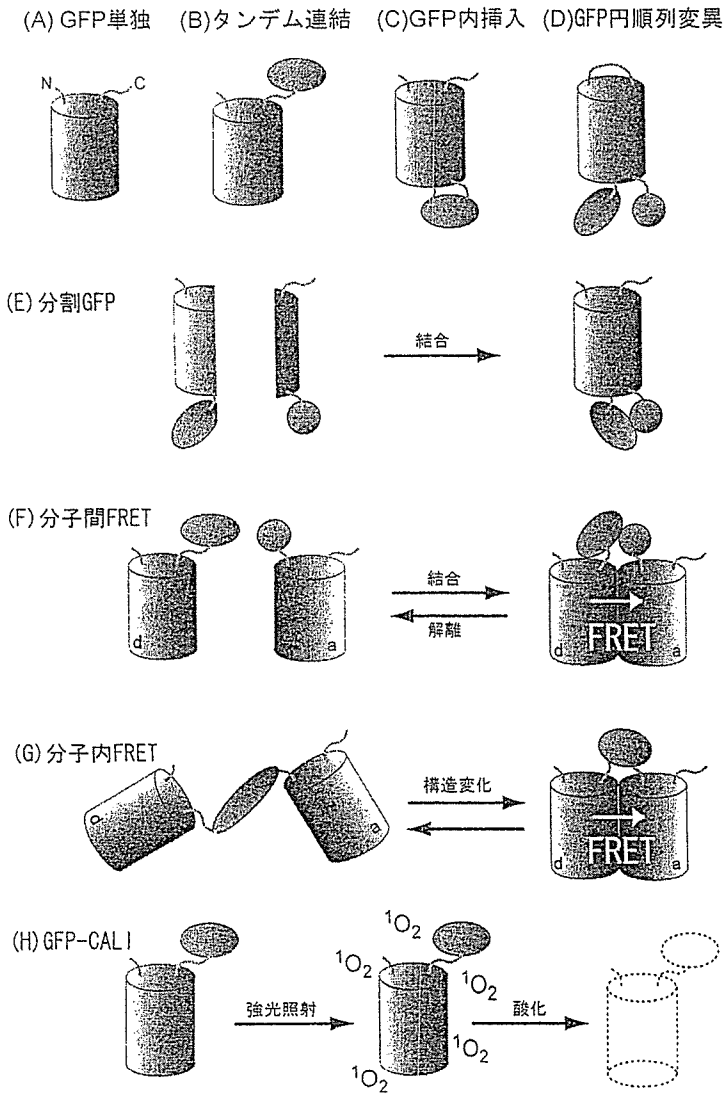

図1 GFPの様々な応用
（A）GFPの単独発現．細胞の蛍光標識などに使われる．
（B）任意のタンパク質とタンデムに連結．細胞内でのタンパク質局在を調べることが可能．
（C）GFP内部に任意のタンパク質を挿入．挿入したタンパク質の構造変化により，GFPの蛍光強度が変化する．
（D）GFP円順列変異体のN末端とC末端に相互作用するタンパク質を連結．それぞれのタンパク質の相互作用によってGFPの励起・蛍光スペクトルが変化する．
（E）GFPをN末端側とC末端側に分割し，それぞれに相互作用するタンパク質を連結．タンパク質相互作用により，蛍光が観察される．
（F）分子間FRET．タンパク質相互作用がない時はドナー(d)を励起するとドナーからの発光が，相互作用がある時はアクセプター（a）からの発光が観察される．
（G）分子内FRET．リン酸化などの修飾によるタンパク質立体構造変化によってFRETの効率が変化する．
（H）蛍光タンパク質を利用した光照射依存的分子不活性化法．強光照射により蛍光タンパク質を介して産生された活性酸素（図中は一重項酸素を表記）が近傍の分子に反応して不活性化する．

みにれびゆう

ものと筆者は信じる．本ミニレビューが少しでも読者の研究にプラスの影響を与えることができれば幸いである．図1にここで紹介した技術をまとめたので参考にされたい．

1) Baird, G.-S., Zacharias, D.-A., & Tsien, R.-Y. (1999) *Proc. Natl. Acad. Sci. USA* 96, 11241-11246
2) Nagai, T., Sawano, A., Park, E.-S., & Miyawaki, A. (2001) *Proc. Natl. Acad. Sci. USA* 98, 3197-3202
3) Kawai, Y., Sato, M., & Umezawa, Y. (2004) *Anal. Chem.* 76, 6144-6149
4) De Angelis, D.-A., Miesenbock, G., Zemelman, B.-V., & Rothman, J.-E. (1998) *Proc. Natl. Acad. Sci. USA* 95, 12312-12316
5) Hu, C.-D., Chinenov, Y., & Kerppola, T.-K. (2002) *Mol. Cell* 9, 789-798
6) Hu, C.-D. & Kerppola, T.-K. (2003) *Nat. Biotechnol.* 21, 539-545
7) Zhang, S., Ma, C., & Chalfie, M. (2004) *Cell* 119, 137-144
8) Ozawa, T., Nogami, S., Sato, M., Ohya, Y., & Umezawa, Y. (2000) *Anal. Chem.* 72, 5151-5157
9) Ozawa, T., Sako, Y., Sato, M., Kitamura, T., & Umezawa, Y. (2003) *Nat. Biotechnol.* 21, 287-293
10) Miyawaki, A., Llopis, J., Hein, R., McCaffery, J.-M., Adams, J.-A., Ikukra, M., & Tsien, R.-Y. (1997) *Nature* 388, 882-887
11) Nagai, T., Yamada, S., Tomita, T., Ichikawa, M., & Miyawaki, A. (2004) *Proc. Natl. Acad. Sci. USA* 101, 10554-10559
12) Nagai, T. & Miyawaki, A. (2004) *Biochem. Biophys. Res. Commun.* 319, 72-77
13) Mank, M., Reiff, D.-F., Heim, N., Friedrich, M.-W., Borst, A., & Griesbeck, O. (2006) *Biophys. J.* 90, 1790-1796
14) Tanabe, T., Oyamada, M., Fujita, K., Dai, P., Tanaka, H., & Takamatsu, T. (2005) *Nat. Methods* 2, 503-505
15) Bulina, M.-E. et al. (0000) *Nat. Biotechnol.* 24, 95-99

永井 健治
(北海道大学電子科学研究所ナノシステム生理学研究部門)

Various applications of fluorescent proteins for cell biology
Takeharu Nagai (Laboratory for Nanosystems Physiology, RIES, Hokkaido University, N12 W6 Kita-ku, Sapporo, Hokkaido 060-0812, Japan)

血管新生を抑制する新規タンパク質 vasohibin

1. はじめに

血管新生（新しい血管網の形成）は，生理的な現象であるが，がんを初めとして様々な病態においても重要な役割を演じていることが明らかになり，血管新生をターゲットとした治療応用に期待が高まっている．血管新生では，周囲の組織との関係を保ちつつ，ヒエラルキー構造を有する秩序だった血管ネットワークを構築する必要がある．それは促進・抑制シグナルの微妙なバランスが巧妙に保たれることで初めて可能になると考えられるが，その詳細な分子メカニズムに関しては不明な点が多い．

2. 血管新生抑制因子

これまで報告されている血管新生の抑制因子は，大きく2群に分類することができる．すなわち遺伝子にコードされている抑制因子と，血管新生とは全く係わりのない分子の分解あるいは代謝によって生じる抑制因子である．前者には，トロンボスポンジン（thrombospondin：TSP），PEDF（pigment epithelium derived factor），マスピン，コンドロモジュリン，IP-10（interferon-γ inducible protein 10），血小板第4因子（platelet factor 4：PF-4）などがある．TSPは，血小板に含有される大分子量の糖タンパク質であるが，さまざまな細胞でも産生・分泌され，細胞外マトリックスに沈着して存在する．TSPには五つのファミリー分子が存在するが，血管新生抑制活性を有しているのはTSP-1とTSP-2であり，腫瘍組織ではTSP-1の発現は減弱する．PEDFとマスピンはセリンプロテアーゼインヒビター（セルピン）スーパーファミリーに属する分子である．このうちPEDFは，網膜色素細胞が産生し，神経の分化に寄与する因子として同定されたが，血管新生抑制活性のあることが判明した．マスピンは，正常乳腺上皮細胞に発現するが，がん化によって発現が消失するもので，がん抑制の活性を有しているが，その一環として血管新生抑制作用が報告された．IP-10とPF-4はケモカインスーパーファミリーに属している．IP-10は，さまざまな細胞でインターフェロンγを初めとして，炎症性の刺激によって誘導される多機能因子であり，その作用の一つとして血管新生抑制作用がある．PF-4は，血小板に含

染色・バイオイメージング実験ハンドブック

細胞や組織の形態・遺伝子・タンパク質を観るための
染色法と顕微鏡観察のすべて

編集／高田邦昭　斎藤尚亮　川上速人

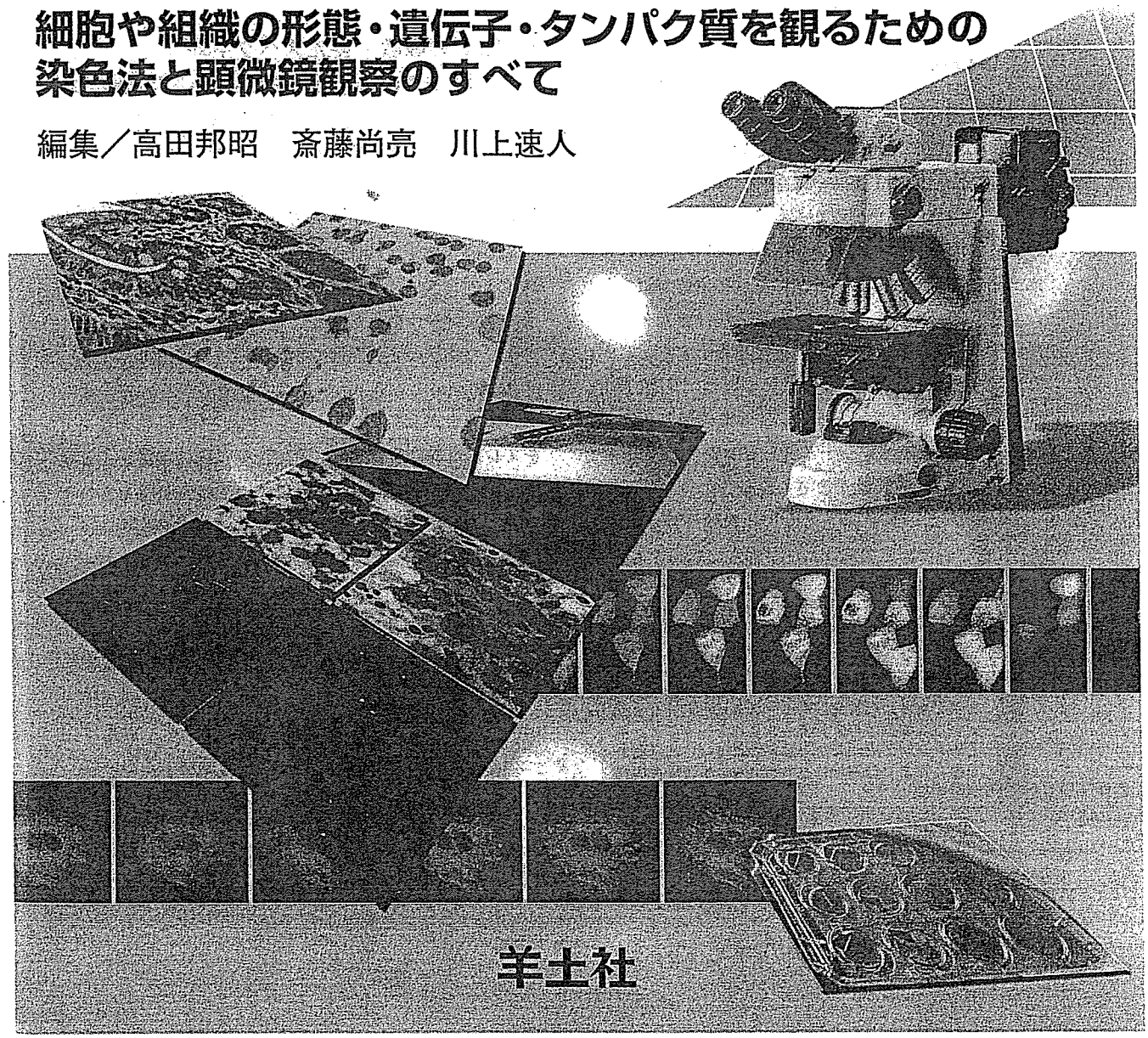

羊土社